Received: 3 August 2020 | Revised: 3 October 2020 | Accepted: 20 October 2020

DOI: 10.1002/ardp.202000282

FULL PAPER

ARCH PHARM DPhG
Archiv der Pharmazie

Novel benzoic acid derivatives: Synthesis and biological evaluation as multitarget acetylcholinesterase and carbonic anhydrase inhibitors

Muharrem Kalaycı[1] | Cüneyt Türkeş[2] | Mustafa Arslan[1] | Yeliz Demir[3] | Şükrü Beydemir[4,5]

[1]Department of Chemistry, Faculty of Arts and Sciences, Sakarya University, Sakarya, Turkey

[2]Department of Biochemistry, Faculty of Pharmacy, Erzincan Binali Yıldırım University, Erzincan, Turkey

[3]Department of Pharmacy Services, Nihat Delibalta Göle Vocational High School, Ardahan University, Ardahan, Turkey

[4]Department of Biochemistry, Faculty of Pharmacy, Anadolu University, Eskişehir, Turkey

[5]The Rectorate of Bilecik Şeyh Edebali University, Bilecik, Turkey

Correspondence

Cüneyt Türkeş, Department of Biochemistry, Faculty of Pharmacy, Erzincan Binali Yıldırım University, 24100 Erzincan, Turkey.
Email: cuneyt.turkes@erzincan.edu.tr

Mustafa Arslan, Department of Chemistry, Faculty of Arts and Sciences, Sakarya University, 54187 Sakarya, Turkey.
Email: marslan@sakarya.edu.tr

Funding information

Research Fund of Erzincan Binali Yildirim University, Grant/Award Number: FBA-2017-501; Research Fund of Ardahan University, Grant/Award Number: 2019-007; Research Fund of Anadolu University, Grant/Award Number: 1610S681; Research Fund of Sakarya University, Grant/Award Number: 2018-2-7-307

Abstract

Alzheimer's disease (AD) is a neurodegenerative disorder characterized by dementia, memory impairment, cognitive dysfunction, and speech impairment. The utility of cholinergic replacement by acetylcholinesterase (AChE) inhibitors in AD treatment has been well documented so far. Recently, studies have also evidenced that human carbonic anhydrases (hCAs) serve as an important target for AD treatment. In this direction, the improvement of new multitarget drugs, which can simultaneously modulate several mechanisms or targets included in the AD pathway, may be a potent strategy to treat AD. In light of these data for understanding and developing AD-related multitarget AChE and hCAs inhibitors, in this study, novel methylene-aminobenzoic acid and tetrahydroisoquinolynyl-benzoic acid derivatives (**4a**–**g** and **6a**–**g**) were designed. The synthesized analogs were experimentally validated for their effects by in vitro and direct enzymatic tests. Also, the compounds were subjected to in silico monitoring with Schrödinger Suite software to assign binding affinities of potential derivatives based on Glide XP scoring, molecular mechanics-generalized Born surface area computing, and validation by molecular docking. The results revealed that **6c** (1,3-dimethyldihydropyrimidine-2,4-(1*H*,3*H*)-dione-substituted, K_I value of 33.00 ± 0.29 nM), **6e** (cyclohexanone-substituted, K_I value of 18.78 ± 0.09 nM), and **6f** (2,2-dimethyl-1,3-dioxan-4-one-substituted, K_I value of 13.62 ± 0.21 nM) from the benzoic acid derivatives in this series were the most promising derivatives, as they exhibited a good multifunctional inhibition at all experimental levels and in the in silico validation against hCA I, hCA II, and AChE, respectively, for the treatment of AD.

KEYWORDS

acetylcholinesterase, carbonic anhydrase, methylene-aminobenzoic acid, tetrahydroisoquinolynyl-benzoic acid

1 | INTRODUCTION

Alzheimer's disease (AD) is one of the most common, rapidly progressive neurodegenerative disorders,[1] which is irreversible, depending on age; it is a cognitive disorder related to aging that is characterized by a decline in language skills, dementia, and memory loss.[2] In the nervous system, acetylcholine (ACh), which is a neurotransmitter, plays an essential role in modulating physiologic and behavioral functions of the cholinergic neurons, and reduced levels of ACh play a vital role in the development of these types of diseases. ACh is hydrolyzed by acetylcholinesterase (AChE; EC 3.1.1.7), and there is a decrease in the level of AChs.[3] AChE is an essential enzyme of nerve impulse transmission. Therefore, AChE inhibition is accepted as one of the most reasonable strategies for the management of AD. Clinically, there are various acetylcholinesterase inhibitors (AChEIs) employed, such as donepezil, galanthamine, rivastigmine, and tacrine (TAC).[4] However, these drugs have shown adverse effects such as nausea, vomiting, diarrhea, dizziness, and hepatotoxicity.[5] Also, they have toxic effects and limited efficacies.[6] For these reasons, novel AChEIs should be synthesized and characterized as more reliable and more efficient for the treatment of AD.

Carbonic anhydrases (CAs; EC 4.2.1.1) are zinc enzymes[7] present in both prokaryotes and eukaryotes,[8] and they catalyze the reversible hydration of CO_2 efficiently to bicarbonate.[9] The α-class CAs are divided into 16 isoforms,[10] which vary in tissue function, kinetic properties, and expression patterns. A characteristic increase or decrease of several CAs activities is related to numerous diseases in human beings. Human carbonic anhydrase I (hCA I) and hCA II play a vital role in a number of pathophysiological processes, such as in respiration,[11] pH and CO_2 homeostasis, secretion, gluconeogenesis, and ureagenesis,[12] which makes them critical drug targets in epilepsy, cerebral edema, and glaucoma.[13] The design of hCA inhibitors (hCAIs) that exhibit both high hCA isoform selectivity and great affinity for the specific disease treatment, without causing an adverse impact owing to off-target hCA modulation, is a challenging goal due to the high structural homology among hCAs.

Some benzoic acid derivatives have active bacteriostatic and fragrant properties, and they are used in the pharmaceutical and perfume industry. These molecules are biologically active and often used as building blocks for drugs or other biologically active molecules, with applications ranging from antibacterial substances to UV protective agents.[14–16] Derivatives of *p*-aminobenzoic acid (PABA) have many interesting pharmacological and biological properties, such as AChEIs in the palliative treatment of AD,[17] antimicrobial activity against Gram-positive bacteria,[18] and inhibitory properties against novel antibacterial,[19] antifungal,[20] and antiviral targets.[21] Furthermore, enaminones undergo significant chemical reactions to construct valuable heterocycles and pharmaceutically essential compounds.[22,23] They possess a wide range of chemical reactions, for instance, pericyclic reactions, Michael addition, C–H functionalization/substitution, and so forth, due to the presence of electrophilic and nucleophilic centers.[24] These compounds are common structural motifs in many bioactive natural products and have significant biological activities, such as anti-inflammatory, antitumor, anticonvulsive, and antibiotic.[25] Furthermore, benzoic acid derivatives are among versatile hCAIs. They are capable of interacting with the hCAs through a variety of inhibition mechanisms, such as coordination with the metal ion, likely as carboxylate anions,[26] anchoring to the Zn-bound H_2O/OH ion,[27] and occluding the entrance of the hCAs' active site cavity.[28] Heterocyclic molecules are one of the most important compounds in drug discovery. They are found in the majority of drugs as synthetic or natural products.[29] Moreover, heterocyclic derivatives containing an oxygen or nitrogen atom have shown interesting biological activities, and they represent important classes of natural and non-natural products.[30] The isoquinoline core in this group is an important heterocyclic moiety that is found in a variety of natural products and pharmaceuticals.[31] The isoquinoline alkaloids are a large family of naturally occurring alkaloids with a wide variety of biological activities, including anti-inflammatory, antimicrobial, antileukemic, and antitumor properties.[32]

Our goal in this study was to incorporate the benzoic acid and the tetrahydroisoquinolynyl scaffolds into one molecule to obtain novel and more potent multitarget AChEIs and hCAIs. Thus, novel methylene-aminobenzoic acid and tetrahydroisoquinolynyl-benzoic acid derivatives (**4a**–**g** and **6a**–**g**) were designed to have the above-mentioned general properties and were synthesized to investigate for their inhibitory effects on AChE and hCA I/II isoenzymes. Afterward, in silico studies, such as toxicity, ADME (absorption, distribution, metabolism, and excretion), and molecular docking, were performed for the optimization of these compounds. The proposed compounds are presented in Scheme 1.

2 | RESULTS AND DISCUSSION

2.1 | Chemistry

Methylene-aminobenzoic acid derivatives were prepared through Mannich three-component synthesis from PABA, 1,3-diketone, and triethyl orthoformate in dimethylformamide (DMF) by heating at 100°C for 3 h. The targeted compounds were synthesized with methylene-aminobenzoic acid derivatives and ethyl cyanoacetate in DMF using potassium *tert*-butoxide for 5 h at room temperature. The prepared compounds (**4a**–**g** and **6a**–**g**) were characterized by ^{1}H nuclear magnetic resonance (NMR), ^{13}C NMR, infrared (IR), and elemental analysis.

From the ^{1}H NMR spectra of the compounds **4a**–**g**, =CH and NH proton peaks on the methylene amino group exhibit resonance at around δ 8.50 and δ 12.50 ppm, respectively. The NH signal was observed to have a downfield shift due to the conjugation and hydrogen bonding. This kind of NH signal has been observed around δ 12.79 ppm.[33] In the ^{13}C NMR spectra, the signals of carbonyl groups, which are ketone, carboxylic acid, ester, and amide, are seen at around δ 194, 167, 165, and 160 ppm, respectively. Whereas α,β-unsaturated carbon atom next to the nitrogen atom exhibits resonance at about δ 140 ppm, the other signal of the α,β-unsaturated carbon atom is seen at around δ 162 ppm. In the infrared spectra of compounds, it was possible to observe the absorptions

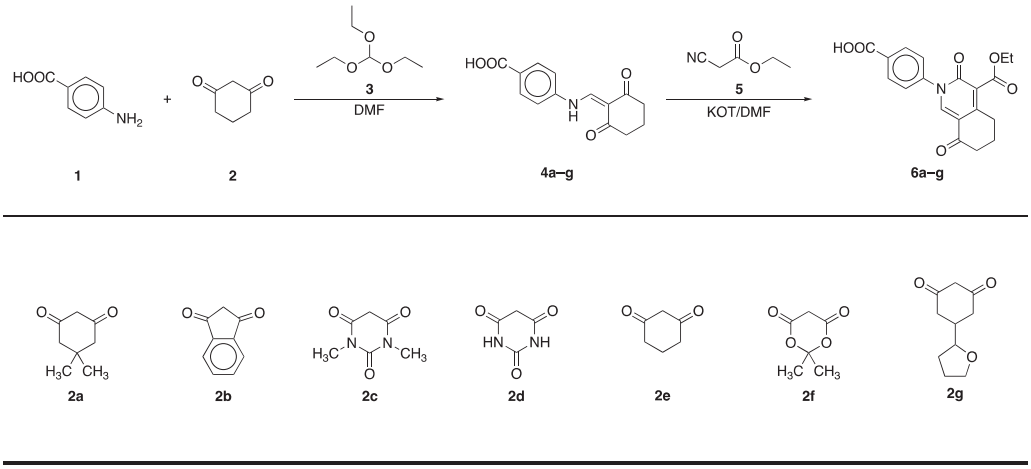

SCHEME 1 A general synthetic procedure for the target derivatives (**4a**–**g** and **6a**–**g**)

around 3450 cm^{-1}, corresponding to ν(N–H) stretchings, absorptions around 1740 cm^{-1}, corresponding to carbonyl moiety, and around 2900–3200 cm^{-1}, corresponding to carboxylic acid–hydrogen stretching. As seen from the ^{1}H NMR spectra of compounds **6a**–**g**, the NH proton signal disappeared due to intramolecular cyclization and one hydrogen atom next to the nitrogen atom in the cyclic structure is observed at δ 8.50 ppm as a singlet resonance. Also, the ν (N–H) stretching of the targeted compounds does not appear anymore from the IR spectra.

2.2 | Biological studies

2.2.1 | AChE activity assay

This study examines the emerging role of AChEIs in the context of AD therapy, together with the in vitro biological evaluation of the AChE inhibitory activity of novel synthesized methylene-aminobenzoic acid and tetrahydroisoquinolynyl-benzoic acid derivatives (**4a**–**g** and **6a**–**g**), compared with the reference drug TAC. The inhibition data for all analogs (**4a**–**g** and **6a**–**g**) are summarized in Tables 1 and 2.

All the synthesized derivatives (**4a**–**g** and **6a**–**g**) exhibited activity in nanomolar levels as inhibitors for the enzyme, with the IC_{50} value in the range of 19.18 ± 0.35 to 33.38 ± 0.40 nM and the K_I value in the range of 13.62 ± 0.21 to 60.76 ± 0.60, compared with TAC as the reference standard agent with a K_I value of 155.29 ± 0.82 nM (2.5–11-fold, approximately). Consequently, the most active compounds of this series were 2,2-dimethyl-1,3-dioxan-4-one derivative **6f**, cyclohexanone derivative **6e**, and 2,3-dihydro-1*H*-inden-1-one analog **6b**, with K_I values of 13.62 ± 0.21, 17.22 ± 0.20, and 20.46 ± 0.24 nM, respectively. In comparison, pyrimidine-2,4,6-(1*H*,3*H*,5*H*)-trione compound **4d** displayed the least activity, with a K_I value of 60.76 ± 0.60 nM. In this respect, it was found that the inhibitory strength order of the novel substituted methylene-aminobenzoic acid and tetrahydroisoquinolynyl-benzoic acid analogs (**4a**–**g** and **6a**–**g**) was as follows: **6f** (2,2-dimethyl-1,3-dioxan-4-one-substituted) > **6e** (cyclohexanone-substituted) > **6b** (2,3-dihydro-1*H*-inden-1-one-substituted) > **4e** (cyclohexane-1,3-dione-substituted) > **4f** (2,2-dimethyl-1,3-dioxane-4,6-dione-substituted) > **4a** (5,5-dimethylcyclohexane-1,3-dione-substituted) > **6d** (dihydropyrimidine-2,4-(1*H*,3*H*)-dione-substituted) > **4g** (5-(tetrahydrofuran-2-yl)cyclohexane-1,3-dione-substituted) > **4b** (1*H*-indene-1,3-(2*H*)-dione-substituted) > **6c** (1,3-dimethyldihydropyrimidine-2,4-(1*H*,3*H*)-dione-substituted) > **6g** (3-(tetrahydrofuran-2-yl)cyclohexan-1-one-substituted) > **6a** (3,3-dimethylcyclohexan-1-one-substituted) > **4c** (1,3-dimethylpyrimidine-2,4,6-(1*H*,3*H*,5*H*)-trione-substituted) > **4d** (pyrimidine-2,4,6-(1*H*,3*H*,5*H*)-trione-substituted).

The discovery of new chemical agents endowed with a potent AChE inhibitory activity is still a relevant subject for AD treatment. In this context, the study by Oliveira et al.[34] was performed with two mitochondriotropic antioxidants, which are catechol and pyrogallol derivative, and hydroxybenzoic acid derivatives, which have longer spacers. The compounds were shown to be potent AChE (IC_{50}s: 7.2 ± 0.5 to 40.5 ± 7.0 μM) and BChE inhibitors (IC_{50}s: 85 ± 5 and 553 ± 22 μM) by a noncompetitive mechanism. Moreover, another study by Oliveira et al.[35] synthesized and screened a small library of benzoic acid-based amide nitrone derivatives against AChE. They found that the *tert*-butyl moiety is the most favorable nitrone pattern in structure–activity relationship studies, and AChE was effectively inhibited by these benzoic acid derivatives that exhibited the noncompetitive inhibition mechanism, with IC_{50} values ranging between 8.3 ± 0.3 and 27.2 ± 2.9 μM. Anand and Singh[36] synthesized and evaluated pyrrolo-isoxazole benzoic acid compounds as potential AChEIs. They investigated the synthesized compounds in vitro against the AChE inhibitory activity in a rat brain homogenate with donepezil, which is a reversible AChEI. All pyrrolo-isoxazole benzoic acid analogs demonstrated a potent AChE inhibitory activity, and most of the derivatives exhibited a similar activity as donepezil (IC_{50} of 21.5 ± 3.2 nM), with IC_{50} values ranging between 7.5 ± 1.5 and 26.9 ± 2.8 nM.

TABLE 1 Inhibition data of AChE and hCA I, II isoenzymes with the synthesized methylene-aminobenzoic acid and tetrahydroisoquinolynyl-benzoic acid derivatives (**4a–g** and **6a–g**), TAC, and AAZ

	AChE		hCA I		hCA II	
Compound ID	K_I (nM)	R^2	K_I (nM)	R^2	K_I (nM)	R^2
4a	22.28 ± 2.39	.9787	37.96 ± 0.28	.9999	65.11 ± 0.47	.9998
4b	32.34 ± 0.45	.9996	70.48 ± 0.65	.9999	75.92 ± 0.52	.9999
4c	56.80 ± 0.80	.9994	47.61 ± 0.36	.9999	27.86 ± 0.24	.9999
4d	60.76 ± 0.60	.9994	163.65 ± 0.92	.9999	51.40 ± 0.39	.9999
4e	21.77 ± 0.27	.9997	50.55 ± 0.47	.9999	49.38 ± 0.49	.9999
4f	22.32 ± 0.34	.9996	35.10 ± 0.18	.9999	108.85 ± 0.66	.9999
4g	31.23 ± 0.57	.9993	37.02 ± 0.27	.9999	60.84 ± 0.33	.9999
6a	50.36 ± 0.45	.9996	74.56 ± 0.53	.9999	46.04 ± 0.15	.9999
6b	20.46 ± 0.24	.9998	59.12 ± 0.47	.9999	99.57 ± 0.29	.9999
6c	38.50 ± 0.35	.9995	33.00 ± 0.29	.9999	59.64 ± 0.20	.9999
6d	24.48 ± 0.41	.9995	41.40 ± 0.25	.9999	22.37 ± 0.07	.9999
6e	17.22 ± 0.20	.9998	62.64 ± 0.37	.9999	18.78 ± 0.09	.9999
6f	13.62 ± 0.21	.9997	51.74 ± 0.40	.9999	33.22 ± 0.17	.9999
6g	41.36 ± 0.48	.9998	47.20 ± 0.37	.9999	32.74 ± 0.10	.9999
TAC	155.29 ± 0.82	.9999	–	–	–	–
AAZ	–	–	439.17 ± 9.30	.9990	98.28 ± 1.69	.9992

Abbreviations: AAZ, acetazolamide; AChE, acetylcholinesterase; hCA, human carbonic anhydrase; TAC, tacrine.

TABLE 2 Selectivity index values for K_I constants of the synthesized methylene-aminobenzoic acid and tetrahydroisoquinolynyl-benzoic acid derivatives (**4a–g** and **6a–g**)

Compound ID	K_I (TAC/AChE)	K_I (AAZ/hCA I)	K_I (AAZ/hCA II)	K_I (hCA I/hCA II)
4a	6.97	11.57	1.51	0.58
4b	4.80	6.23	1.29	0.93
4c	2.73	9.23	3.53	1.71
4d	2.56	2.68	1.91	3.18
4e	7.13	8.69	1.99	1.02
4f	6.96	12.51	0.90	0.32
4g	4.97	11.86	1.62	0.61
6a	3.08	5.89	2.13	1.62
6b	7.59	7.43	0.99	0.59
6c	4.03	13.31	1.65	0.55
6d	6.34	10.61	4.39	1.85
6e	9.02	7.01	5.23	3.34
6f	11.40	8.49	2.96	1.56
6g	3.75	9.30	3.00	1.44

Abbreviations: AAZ, acetazolamide; AChE, acetylcholinesterase; hCA, human carbonic anhydrase; TAC, tacrine.

2.2.2 | CA activity assay

This study also sheds light on the novel synthesized methylene-aminobenzoic acid and tetrahydroisoquinolynyl-benzoic acid derivatives in terms of hCAIs. Initially, hCA I and II isoforms were purified from human erythrocytes by using rapid and simple chromatographic methods. Subsequently, reported methylene-aminobenzoic acid and tetrahydroisoquinolynyl-benzoic acid analogs (**4a–g** and **6a–g**) were analyzed in vitro for their inhibitory properties against the physiologically relevant hCA isoforms I and II, compared with acetazolamide (AAZ). AAZ, which is a noncompetitive inhibitor of hCAs and used as a reference drug in the assays, is a sulfonamide derivative with anticonvulsant, antiglaucoma, and diuretic properties.[37] The inhibition data and selectivity index (S_I) values for all derivatives (**4a–g** and **6a–g**) are presented in Tables 1 and 2.

Regarding the inhibition of the cytosolic isoform hCA I, it was observed that the analyzed analogs (**4a–g** and **6a–g**) exhibited inhibition with IC_{50} values ranging between 20.10 ± 0.46 and 56.74 ± 1.70 nM, and K_I values ranging between 33.00 ± 0.29 and 163.65 ± 0.92 nM. Moreover, all compounds (**6a–g**) showed a higher activity than the reference compound AAZ (K_I of 439.17 ± 9.30 nM). Derivative **6c** carrying the 1,3-dimethyldihydropyrimidine-2,4-(1*H*,3*H*)-dione moiety (K_I of 33.00 ± 0.29 nM) was found to be the most potent agent, whereas pyrimidine-2,4,6-(1*H*,3*H*,5*H*)-trione-substituted analog **4d** (K_I of 163.65 ± 0.92 nM) had the lowest activity against cerebral and retinal edema-linked isoform hCA I. Furthermore, cyclohexanone-substituted compound **6e** (K_Is for hCA I

and hCA II 62.64 ± 0.37 and 18.78 ± 0.09 nM, respectively) was found as the most selective hCA I inhibitor with an S_I value (hCA I/hCA II) of 3.34. The hCA I inhibitory activities of the newly substituted methylene-aminobenzoic acid and tetrahydroisoquinolynyl-benzoic acid analogs (**4a**–**g** and **6a**–**g**) reduced in the following order: **6c** (1,3-dimethyldihydropyrimidine-2,4-(1*H*,3*H*)-dione-substituted) > **4f** (2,2-dimethyl-1,3-dioxane-4,6-dione-substituted) > **4g** (5-(tetrahydrofuran-2-yl)cyclohexane-1,3-dione-substituted) > **4a** (5,5-dimethylcyclohexane-1,3-dione-substituted) > **6d** (dihydropyrimidine-2,4-(1*H*,3*H*)-dione-substituted) > **6g** (3-(tetrahydrofuran-2-yl)cyclohexan-1-one-substituted) > **4c** (1,3-dimethylpyrimidine-2,4,6-(1*H*,3*H*,5*H*)-trione-substituted) > **4e** (cyclohexane-1,3-dione-substituted) > **6f** (2,2-dimethyl-1,3-dioxan-4-one-substituted) > **6b** (2,3-dihydro-1*H*-inden-1-one-substituted) > **6e** (cyclohexanone-substituted) > **4b** (1*H*-indene-1,3-(2*H*)-dione-substituted) > **6a** (3,3-dimethylcyclohexan-1-one-substituted) > **4d** (pyrimidine-2,4,6-(1*H*,3*H*,5*H*)-trione-substituted).

The other cytosolic isoform hCA II, which is known to be linked with edema, epilepsy, and glaucoma, was potently inhibited in nanomolar levels by all the newly synthesized methylene-aminobenzoic acid and tetrahydroisoquinolynyl-benzoic acid analogs (**4a**–**g** and **6a**–**g**), with IC_{50} values in the range of 19.75 ± 0.90 to 45.10 ± 0.74 nM and K_I values in the range of 18.78 ± 0.09 to 108.85 ± 0.66 nM. Also, except for compounds **4f** and **6b**, which displayed better inhibition than AAZ, all other derivatives were found to be highly potent inhibitors as compared with clinically used reference agent AAZ (K_I of 98.28 ± 1.69 nM).

Compound **6e** bearing the cyclohexanone moiety was the most potent inhibitor of the second abundant isoform hCA II with a K_I value of 18.78 ± 0.09 nM; dihydropyrimidine-2,4-(1*H*,3*H*)-dione-substituted tetrahydroisoquinolynyl-benzoic acid analog **6d** with a K_I value of 22.37 ± 0.07 nM was the second most potent inhibitor; and 1,3-dimethylpyrimidine-2,4,6-(1*H*,3*H*,5*H*)-trione-substituted derivative **4c** was the third most potent inhibitor with a K_I value of 27.86 ± 0.24 nM. Moreover, it is worth mentioning that the inhibitory effect of compound **4f** on hCA II was selective with an S_I value (hCA I/hCA II) of 0.32, and the 2,2-dimethyl-1,3-dioxane-4,6-dione substituent enhanced the potency and selectivity against hCA II. The order of inhibition activities of the new substituted methylene-aminobenzoic acid and tetrahydroisoquinolynyl-benzoic acid analogs (**4a**–**g** and **6a**–**g**) against hCA II decreased as follows: **6e** (cyclohexanone-substituted) > **6d** (dihydropyrimidine-2,4-(1*H*,3*H*)-dione-substituted) > **4c** (1,3-dimethylpyrimidine-2,4,6-(1*H*,3*H*,5*H*)-trione-substituted) > **6g** (3-(tetrahydrofuran-2-yl)cyclohexan-1-one-substituted) > **6f** (2,2-dimethyl-1,3-dioxan-4-one-substituted) > **6a** (3,3-dimethylcyclohexan-1-one-substituted) > **4e** (cyclohexane-1,3-dione-substituted) > **4d** (pyrimidine-2,4,6-(1*H*,3*H*,5*H*)-trione-substituted) > **6c** (1,3-dimethyldihydropyrimidine-2,4-(1*H*,3*H*)-dione-substituted) > **4g** (5-(tetrahydrofuran-2-yl)cyclohexane-1,3-dione-substituted) > **4a** (5,5-dimethylcyclohexane-1,3-dione-substituted) > **4b** (1*H*-indene-1,3-(2*H*)-dione-substituted) > **6b** (2,3-dihydro-1*H*-inden-1-one-substituted) > **4f** (2,2-dimethyl-1,3-dioxane-4,6-dione-substituted).

Compounds **6f, 6c**, and **6e** were the most active in the AChE and hCA I, II isoenzymes' inhibition, respectively; however, their analogs **4f, 4c**, and **4e** showed less activity than compounds **6f, 6c**, and **6e**. This enhanced selectivity toward AChE may be related to the hydrophobic interaction between Tyr337 and the pyridine ring of compound **6f**. Furthermore, selectivity for hCA I and II isoenzymes may be attributed to the carboxyl group of the pyridine ring of derivative **6c**, which formed an H-bond (distance: 2.12 Å) with Gln92, and the carboxyl groups of compound **6e** formed two H-bonds (distances: 2.01 and 1.77 Å) with Asn62 and Ans67. Thus, these results reveal the importance of heterocyclic fragment.

A vast majority of hCAIs, such as AAZ, brinzolamide, dichlorphenamide, and methazolamide, utilize a sulfonamide functionality to bind with the Zn ion, displacing the water nucleophile and ultimately anchoring the inhibitor in the binding site. Lately, different new classes of inhibitors have been identified, such as the carboxylic acids, the coumarins, the phenols, the polyamines, the thiazoles, the pyrazoles, the pyrazolines, and antiepileptic drugs.[26,38–43] These ligand structures treat not by directly coordinating to the catalytic zinc ion but by either composing the H-bond with the amino acids, or interacting with the hydrophobic amino acid residues in the binding pocket, or both. Hereby, this indirect interaction has the potential for developing isoform-specific hCAIs, which was quite difficult with sulfonamide-based inhibitors,[44] as in this study.

In this direction, many recent studies have found that benzoic acid derivatives exhibit effective inhibition such as sulfonamides, which are potent hCAIs. Rotondi et al.[40] synthesized and analyzed 2-(benzylsulfinyl)benzoic acid derivatives as innovative and atypical inhibitors against four different isoenzymes of hCA (hCA I, II, IX, and XII). They determined that all the evaluated analogs had no affinity for the common off-target hCA I isoenzyme (K_I > 100 μM), and some of them were more active against the tumor-related isoenzyme hCA IX when compared with the parent agent 2-(benzylsulfinyl)benzoic acid. Innocenti et al.[45] reported the inhibition of 12 mammalian isoenzymes of the metalloenzyme hCA I–XIV, with a series of phenols investigated. The inhibition profile of these hCAIs was different from that of the sulfonamide derivatives, the main class of clinically used inhibitors. They showed that 2- and 4-hydroxybenzoic acid derivatives were generally effective low micromolar hCAIs, with K_I values in the range of 7.1–885 and 4.8–809 μM against hCA I–XIV, respectively. Martin and Cohen[46] investigated hydroxybenzoic acids to determine whether they represent a new class of nonmetal-binding inhibitors of hCA II. They were determined to be a viable alternative to direct Zn(II) binding for the inhibition of these metalloenzymes of the bound nucleophile, and these fragments inhibit hCA II with IC_{50} values in the low millimolar range.

2.3 | In silico studies

2.3.1 | Absorption, distribution, metabolism, excretion, and toxicity (ADME–Tox) study

The molecular weights (MWs, 287.32–425.44) and dipole moments (dipole, 2.18–8.35) of the methylene-aminobenzoic acid and

tetrahydroisoquinolynyl-benzoic acid compounds (**4a**–**g** and **6a**–**g**) have been reported to be in the permissible value range. Volume (774.46–1315.30), which is the total solvent-accessible volume descriptor, was determined to be in the permissible range for these target analogs (**4a**–**g** and **6a**–**g**), compared with reference values. The log*P* values, such as QPlog*P*oct, QPlog*P*w, QPlog*P*o/w, QPlog*S*, QPlogHERG, QPlogBB, QPlog*K*p, and QPlog*K*hs, range from 13.80 to 23.51, 9.87 to 16.08, 12.76 to 16.08, −5.29 to −2.19, −4.29 to −2.30, −2.82 to −1.37, −6.61 to −3.91, and −0.76 to −0.21, respectively, indicating that these analogs (**4a**–**g** and **6a**–**g**) have a high capacity. The values of human oral absorption (HOA) range between 36.03% and 72.26%, and the van der Waals surface area of polar nitrogen and oxygen atoms (PSA) is in the range of 114.32–194.14, indicating that all derivatives (**4a**–**g** and **6a**–**g**) had the acceptable values. All the analogs (**4a**–**g** and **6a**–**g**) have displayed poor Caco-2 cell permeability values (except for compounds **4a**, **4e**, **4g**, and **6f**; QPPCaco, 2.25–53.45) and Madin–Darby canine kidney (MDCK) cell permeability values (except for compound **6f**; QPPMDCK, 0.87–26.54). Indeed, all newly synthesized methylene-aminobenzoic acid and tetrahydroisoquinolynyl-benzoic acid derivatives (**4a**–**g** and **6a**–**g**) displayed good drug-like properties with zero violation of Lipinski's rule, one violation of the Jorgensen's rule (except for compounds **4a**–**b**, **4e**, **4g**, and **6f**), and zero pan-assay interference compounds (PAINS) alerts (except for compounds **4b**–**d** and **4f**; Table 3). Moreover, the ADME–Tox values calculated for 2, 2-dimethyl-1,3-dioxan-4-one-substituted compound **6f** might explain why, being a potent AChE inhibitor, this ligand has the most AChE inhibitory activity in biological experiments (Figure S1).

2.3.2 | Molecular docking study

To better evaluate the molecular basis of the binding affinities of the novel synthesized methylene-aminobenzoic acid and tetrahydroisoquinolynyl-benzoic acid derivatives (**4a**–**g** and **6a**–**g**), the most efficient inhibitors **6c** ($C_{19}H_{17}N_3O_7$), **6e** ($C_{19}H_{17}NO_6$), and **6f** ($C_{19}H_{19}NO_7$) against the hCA I, II, and AChE were docked into the active sites of these enzymes. The docking results were compared with co-crystallized natural ligands GZH ($C_{16}H_{15}ClF_3N_3O_3S$), GTQ ($C_7H_6O_4$), and HI6 ($C_{14}H_{16}N_4O_3$) at the binding sites of the receptors (6I0L, 4E3D, and 5HF9, respectively). The molecular docking was performed using 6I0L (CA I complexed with GZH, resolution of 1.40 Å, species: *Homo sapiens*), 4E3D (CA II complexed with GTQ, resolution of 1.60 Å, species: *Homo sapiens*), and 5HF9 (AChE complexed with HI6, resolution of 2.20 Å, species: *Homo sapiens*). The green lines display hydrophobic interactions, whereas the pink line exhibits the hydrogen bond interaction. For validation of the in silico molecular docking procedure, the co-crystalized ligands (GZH, GTQ, and HI6) in chain A were extracted and redocked into the binding sites. To evaluate the quality of the co-crystallized ligands, their root mean square deviation (RMSD) scores were computed. The results were compared with reference compounds derived from the corresponding 6I0L, 4E3D, and 5HF9, and the docking poses were superimposed. As expected, RMSD scores were computed as <2 Å, that is, 1.11, 0.17, and 0.95 Å, respectively.

In the present in silico docking study, the docking pattern of HI6 was compared with analog **6f** (K_I of 13.62 ± 0.21 nM for AChE), which is the most active derivative of the new methylene-aminobenzoic acid and tetrahydroisoquinolynyl-benzoic acid series. According to the literature, the native ligand HI6 forms an H-bond (distance 2.14 Å) with Phe295 in the catalytic domain of 5HF9. Moreover, HI6 forms both π–π stacking and π–cation interactions with Tyr124, Trp286, and Tyr341, and only π–π stacking interaction with Trp72 (Figure S2). Additionally, the interaction of this pharmacophore, which resides in the AChE, reveals that 2,2-dimethyl-1,3-dioxan-4-one-substituted derivative **6f** formed two H-bond (distances: 1.99 and 2.67 Å) interactions with Trp286 and Arg296 and hydrophobic interactions with Tyr86 and Tyr337, and the docking scores of HI6 (molecular mechanics-generalized Born surface area [MM-GBSA] value of −90.85 kcal/mol) and analog **6f** (MM-GBSA value of −40.516 kcal/mol) are shown to be −13.59 and −8.03, respectively. Furthermore, the most prominent residues accommodating hydrophobic fragments include Tyr86, Trp286, and Tyr337, as well as Tyr72, Val73, Pro88, Tyr124, Val294, Phe295, Phe297, Phe338, and Tyr341 (Figure 1).

The molecular understanding of the binding of 6I0L with the macrodomain revealed that hCA I residues Phe91, Gln92, His94, His96, Glu106, His119, Ala121, Leu131, Ala135, Leu141, Val143, Ser197, Leu198, Thr199, His200, Pro202, Val207, and Trp209 act as the critical amino acids in the binding site, which form molecular interactions with GZH. In this direction, GZH, which is reported as a natural ligand, and compound **6c** (K_I of 133.00 ± 0.29 nM for hCA I), which has the most potent inhibitory activity among the newly methylene-aminobenzoic acid and tetrahydroisoquinolynyl-benzoic acid analogs (**4a**–**g** and **6a**–**g**), were analyzed in terms of contacts with hCA I. The native ligand GZH forms two H-bonds (distances: 1.91 and 1.93 Å) with Thr199. Apart from this, GZH forms π–π interaction with His94. Also, it plays a reference role as a Zn-binding moiety with the hCA I by forming a coordinate bond with Zn(II) ion (Figure S3). The 1, 3-dimethyldihydropyrimidine-2,4-(1*H*,3*H*)-dione-substituted derivative of tetrahydroisoquinolynyl-benzoic acids (**6c**) formed two strong H-bonds (distances: 2.12 and 1.93 Å) with Gln92 and Thr199, respectively. Meanwhile, hydrophobic interactions were observed between derivative **6c** and Phe91, Ala121, Leu131, Ala132, Ala135, Val143, Leu198, Pro202, Tyr204, and Trp209 (Figure 2). XP glide docking of analog **6c** with the active domain of 6I0L showed a higher docking score of −7.28 kcal/mol and an MM-GBSA value of −33.65 kcal/mol, compared with GZH with a docking score of −6.39 kcal/mol and an MM-GBSA value of −17.37 kcal/mol.

A further look into the crystallographic structural features between 4E3D and native ligand GTQ revealed, is involved in two H-bonds (distances: 2.33 and 2.39 Å) with Thr199 and Thr200 residues, respectively (Figure S4). Figure 3 depicts the simulated

TABLE 3 ADME–Tox-related parameters of the methylene-aminobenzoic acid and tetrahydroisoquinolynyl-benzoic acid derivatives (**4a–g** and **6a–g**)

Principal descriptors	4a	4b	4c	4d	4e	4f	4g	6a	6b	6c	6d	6e	6f	6g	Standard range
MW	287.32	293.28	303.27	275.22	259.26	291.26	329.35	383.40	389.36	399.36	371.31	355.35	373.36	425.44	130.0 to 725.0
Dipole	4.49	4.43	5.24	5.47	4.42	5.21	6.13	4.50	4.15	4.05	2.18	4.24	7.59	8.35	1.0 to 12.5
Volume	923.09	921.24	930.70	774.46	849.37	903.31	1086.89	1190.55	1167.45	1182.79	1067.98	1115.77	1158.35	1315.30	500.0 to 2000.0
QPlog*P*oct	14.88	15.66	15.16	16.44	13.80	15.80	18.02	20.45	20.82	21.21	20.72	19.34	19.85	23.51	8.0 to 35.0
QPlog*P*w	9.87	11.23	10.21	13.35	9.88	12.00	11.88	13.54	14.64	15.29	16.08	13.56	12.76	15.49	4.0 to 45.0
QPlog*P*o/w	1.95	1.95	2.02	0.21	1.42	0.84	2.17	2.08	2.08	1.19	0.48	1.58	2.46	2.07	−2.0 to 6.5
QPlog*S*	−3.06	−3.52	−3.56	−2.19	−2.84	−2.56	−4.60	−4.50	−4.56	−4.12	−3.84	−4.25	−4.79	−5.29	−6.5 to 0.5
QPlogHERG	−2.43	−3.98	−3.13	−2.30	−2.85	−2.90	−3.89	−3.31	−4.29	−3.61	−3.42	−3.59	−3.71	−4.03	Concern below −5
QPPCaco	34.66	23.73	14.96	3.74	29.25	21.08	31.09	16.59	15.07	8.60	2.25	15.15	53.45	14.85	<25 poor; great > 500
QPlogBB	−1.37	−1.72	−1.91	−2.20	−1.55	−1.70	−1.83	−1.89	−2.01	−2.29	−2.82	−2.02	−1.46	−2.20	−3.0 to 1.2
QPPMDCK	16.62	11.03	6.70	1.50	13.83	9.71	14.77	7.49	6.75	3.68	0.87	6.79	26.54	6.65	< 25 poor; great > 500
QPlog*K*p	−4.20	−3.91	−4.90	−6.07	−4.35	−4.63	−4.29	−4.95	−4.48	−5.48	−6.61	−5.01	−3.93	−5.02	−8.0 to −1.0
QPlog*K*hsa	−0.32	−0.35	−0.33	−0.64	−0.53	−0.76	−0.29	−0.22	−0.29	−0.55	−0.54	−0.42	−0.21	−0.28	−1.5 to 1.5
HOA	65.92	62.96	59.77	38.42	61.52	55.56	66.38	60.96	60.20	50.62	36.03	57.34	72.26	60.04	<25% poor; high > 80%
PSA	114.32	118.98	143.19	172.22	115.05	133.34	123.33	137.05	138.73	164.63	194.14	138.13	124.30	146.01	7.0 to 200.0
Rule of five	0	0	0	0	0	0	0	0	0	0	0	0	0	0	Max. 4
Rule of three	0	0	1	1	0	1	0	1	1	1	1	1	0	1	Max. 3
PAINS	0	1	1	1	0	1	0	0	0	0	0	0	0	0	–

Abbreviations: Dipole, computed dipole moment of the compound; HOA, human oral absorption; MW, molecular weight of the compound; PAINS, pan-assay interference compounds; PSA, van der Waals surface area of polar nitrogen and oxygen atoms; QPlogBB, brain/blood partition coefficient; QPlogHERG; IC_{50} value for blockage of HERG K^+ channels; QPlog*K*p, skin permeability; QPlog*K*hsa, prediction of binding to human serum albumin; QPlog*P*oct, octanol/gas partition coefficient; QPlog*P*w, water/gas partition coefficient; QPlog*P*o/w, octanol/water partition coefficient; QPPCaco, apparent Caco-2 cell permeability in nm/s; QPPMDCK, apparent MDCK cell permeability in nm/s; QPlog*S*, aqueous solubility; Rule of three, number of violations of Jorgensen's rule of three; Rule of five, number of violations of Lipinski's rule of five; Volume, total solvent-accessible volume in $Å^3$ using a probe with a 1.4-Å radius.

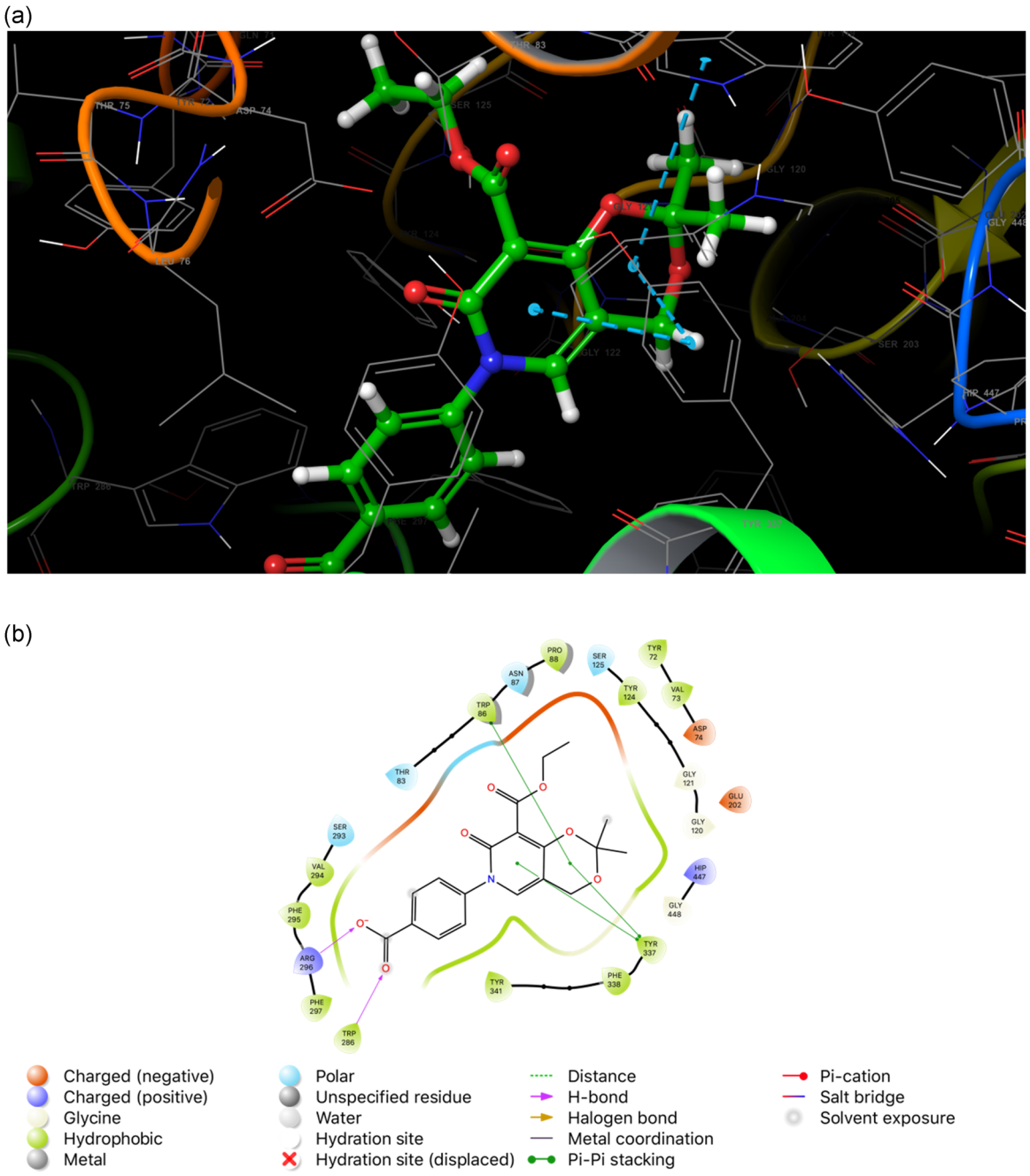

FIGURE 1 Molecular docking of acetylcholinesterase (PDB ID: 5HF9; chain A) with derivative **6f** ($C_{19}H_{19}NO_7$: 4-[8-(ethoxycarbonyl)-2, 2-dimethyl-7-oxo-4*H*-(1,3)-dioxino-(5,4-*c*)-pyridin-6-(7*H*)-yl]benzoic acid). (a) A three-dimensional ligand interaction diagram of 5HF9 with derivative **6f**. (b) Two-dimensional docking pose of derivative **6f** with the key amino acids within the binding pocket of 5HF9

binding pose of the most active cyclohexanone-substituted analog **6e** (K_I of 18.78 ± 0.09 nM for hCA II). The carboxyl groups formed four strong H-bonds (distances: 2.49, 2.01, 1.77, and 2.09 Å) with Trp5, Asn62, Ans67, and Thr199, respectively. However, His94 was observed to be stacked toward the benzene ring, displaying face-to-face interaction. It also formed a hydrophobic interaction with Trp5, Leu60, Leu198, Pro201, and Pro202. GTQ with a docking score of −6.13 kcal/mol and derivative **6e** with a higher docking score of −8.34 kcal/mol displayed different interactions, and the MM-GBSA values were computed to be −17.61 and −29.43 kcal/mol, respectively.

These molecular docking results provide insights into the ligand–protein interactions. They rationalized the experimental data, confirming that the binding modes of the most active derivatives in series (**6f**, **6c**, and **6e**) against AChE and hCA isoforms I, II have the most favorable binding free energy.

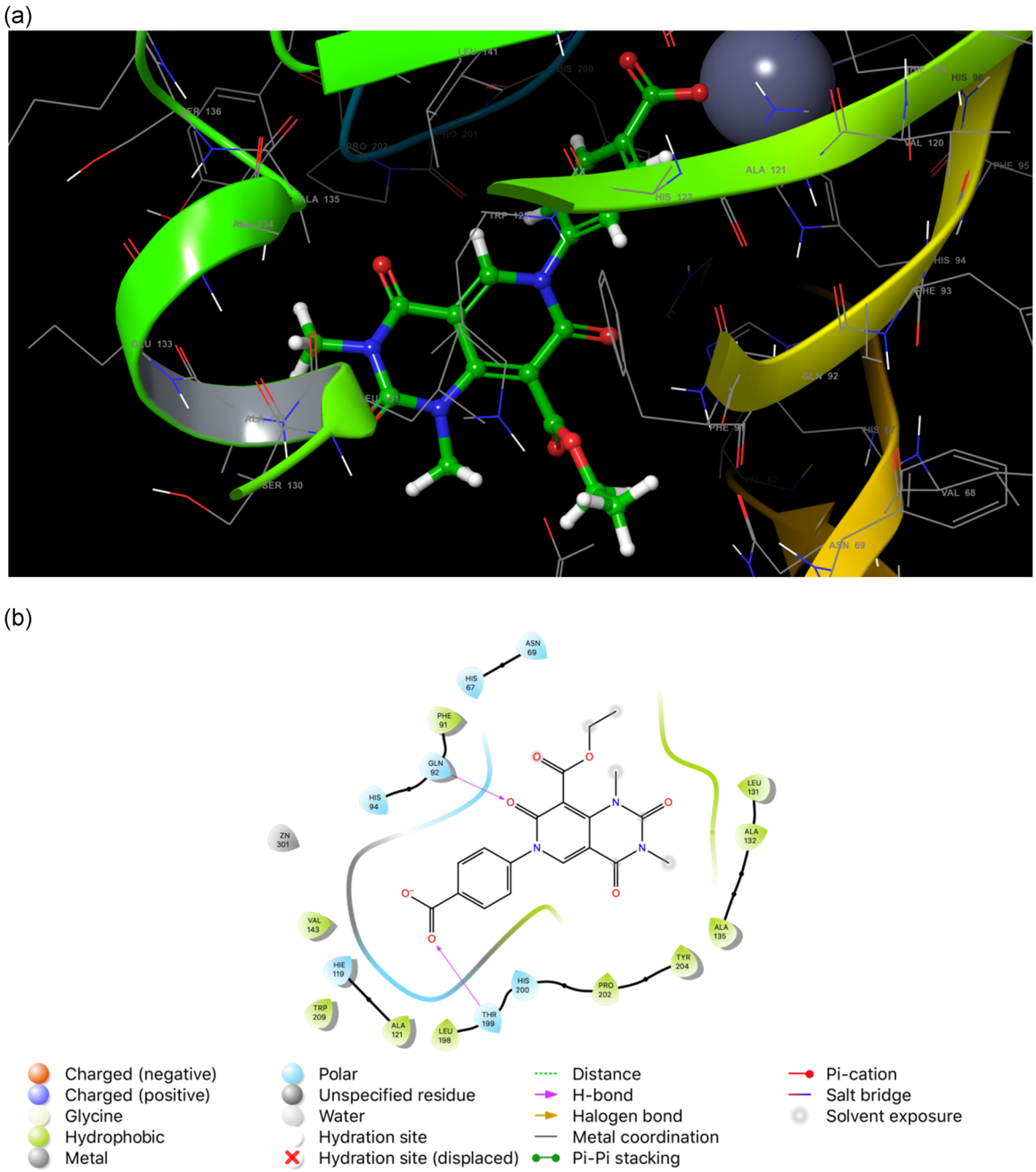

FIGURE 2 Molecular docking of human carbonic anhydrase I (PDB ID: 6I0L; chain A) with derivative **6c** ($C_{19}H_{17}N_3O_7$: 4-[8-(ethoxycarbonyl)-1,3-dimethyl-2,4,7-trioxo-1,3,4,7-tetrahydropyrido-(4,3-*d*)-pyrimidin-6-(2*H*)-yl]benzoic acid). (a) A three-dimensional ligand interaction diagram of 6I0L with derivative **6c**. (b) Two-dimensional docking pose of derivative **6c** with the key amino acids within the binding pocket of 6I0L

3 | CONCLUSION

In this study, new methylene-aminobenzoic acid and tetrahydroisoquinolynyl-benzoic acid derivatives (**4a–g** and **6a–g**) were designed and synthesized as innovative hCAIs, and the structures of the compounds were elucidated by IR, ^{1}H NMR, and ^{13}C NMR spectral data. All the final compounds, **4a–g** and **6a–g**, were monitored in vitro for their inhibitory potential against AChE and hCA I, II isoenzymes. The biological studies, which were determined as significant targets in AD treatment, primarily, were performed using Ellman's and Verporte's methods. It also was investigated, by in silico screening, the ligand–receptor interactions and druggability of these analogs utilizing Schrödinger Suite software, which confirmed the obtained activity. In vitro studies revealed that the synthesized compounds (**4a–g** and **6a–g**) based on our design notably inhibited hCA I, hCA II (except for

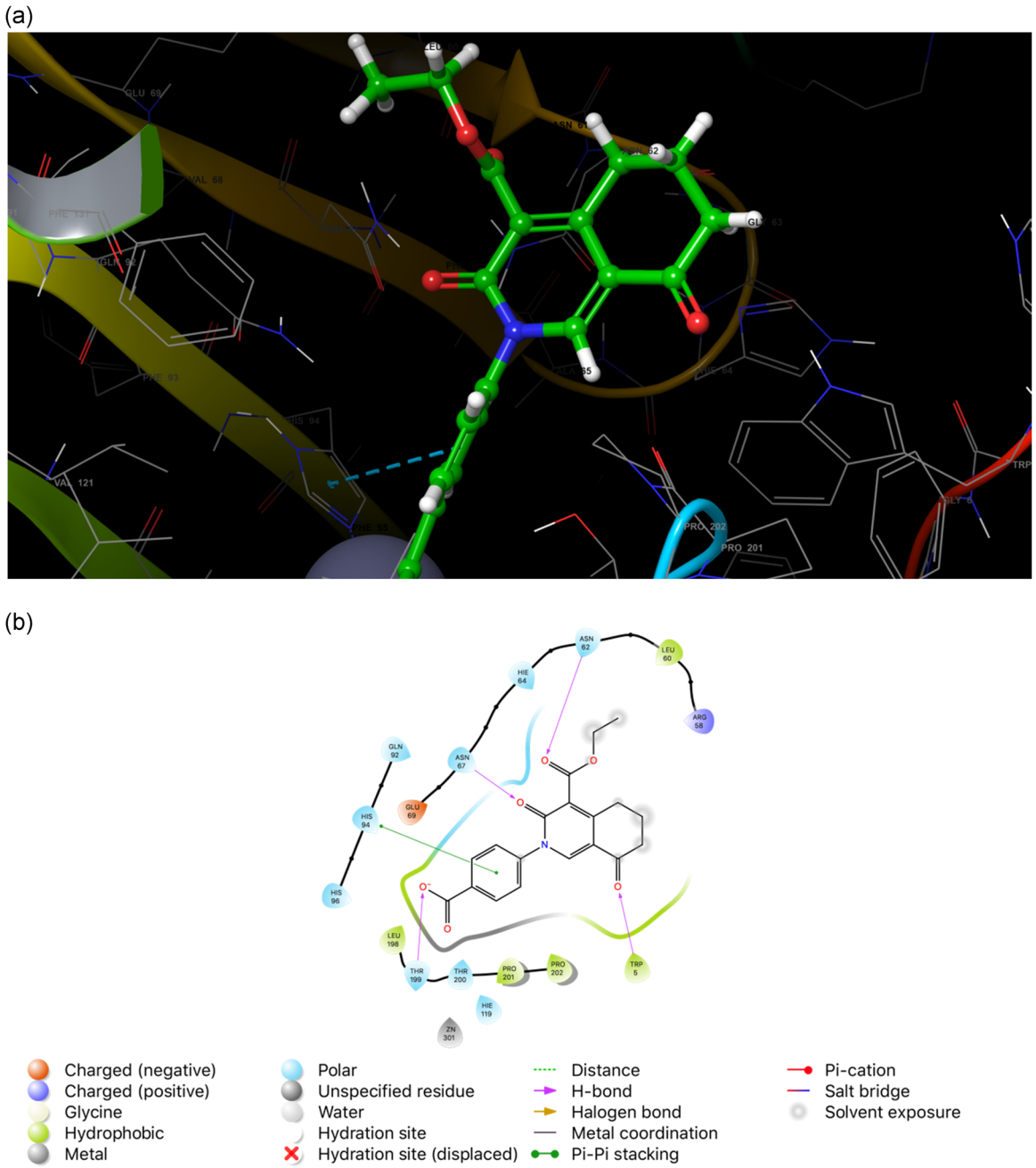

FIGURE 3 Molecular docking of human carbonic anhydrase II (PDB ID: 4E3D; chain A) with derivative **6e** ($C_{19}H_{17}NO_6$: 4-[4-(ethoxycarbonyl)-3,8-dioxo-5,6,7,8-tetrahydroisoquinolin-2-(3*H*)-yl]benzoic acid). (a) A three-dimensional ligand interaction diagram of 4E3D with derivative **6e**. (b) Two-dimensional docking pose of derivative **6e** with the key amino acids within the binding pocket of 4E3D

compounds **4f** and **6b**), and AChE, even more than reference drugs, namely AAZ and TAC. In this series, derivative **6c** with the 1,3-dimethyldihydropyrimidine-2,4-(1*H*,3*H*)-dione substitution inhibited hCA I with the lowest K_I value, whereas derivative **6e** with cyclohexanone substitution was determined as the most selective hCA I inhibitor. Additionally, analog **6e** exhibited the most potent inhibition against hCA II. Besides, derivative **6f** with the 2,2-dimethyl-1,3-dioxan-4-one substitution was defined as the most significant and selective AChE inhibitor in this series. Furthermore, the ADME–Tox study revealed that all the derivatives had good oral bioavailability with respect to Lipinski's rule of five, Jorgensen's rule of three, and PAINS. Finally, there is a need to find an effective way to treat AD, because its complex mechanisms have not been entirely described. All derivatives (**4a–g** and **6a–g**) in this series can be considered as outstanding multitarget inhibitors for further investigations in AD treatment.

4 | EXPERIMENTAL

4.1 | Chemistry

4.1.1 | General

Melting points were determined by a Yanagimoto micro-melting point apparatus and were uncorrected. IR spectra were acquired on a SHIMADZU Prestige-21 (200 VCE) spectrometer (Shimadzu). ^{1}H and ^{13}C NMR spectra were acquired on a VARIAN Infinity Plus spectrometer in 300 and 75 Hz, respectively (Varian, Inc.). ^{1}H and ^{13}C chemical shifts are referenced to the internal deuteranated solvent. The elemental analysis was carried out with a Leco CHNS-932 instrument (Leco Corp.). All chemicals were purchased from Sigma-Aldrich Chemie GmbH.

The InChI codes of the investigated compounds, together with some biological activity data, are provided as Supporting Information.

4.1.2 | General procedure for the preparation of the methylene-aminobenzoic acid derivatives 4a–g

1,3-Diketone (1 mmol), *p*-aminobenzoic acid (1 mmol), and triethylorthoformate (1.5 mmol) in DMF were heated at 100°C for 3 h. After completion of the reaction, the reaction mixture was cooled to room temperature and ice-cold water was added to the reaction flask. The mixture was acidified by HCl and the precipitate was filtered by vacuum filtration. Then, it was washed with water and dried in a vacuum oven. The product was purified by crystallization in acetone.

*4-{[(4,4-Dimethyl-2,6-dioxocyclohexylidene)methyl]amino}benzoic acid (**4a**)*

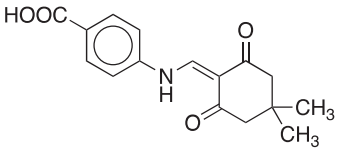

Yield 72%, m.p. 264–265°C; IR (ν, cm^{-1}): 3453 (N–H), 3200–2900 (COO–H), 3092 (=C–H), 1748 (C=O); ^{1}H NMR (300 MHz, dimethyl sulfoxide [DMSO]): δ 12.60 (d, 1H), 8.50 (d, 1H), 7.93 (d, 2H), 7.57 (d, 2H), 2.42 (t, 3H), 2.06 (s, 1H), 0.97–0.92 (m, 6H); ^{13}C NMR (75 MHz, DMSO): δ 194.03, 167.29, 164.33, 161.12, 159.60, 141.82, 132.26, 131.50, 129.18, 118.62, 112.43, 61.36, 49.87, 33.22, 28.26, 14.80. Calculated for $C_{16}H_{17}NO_4$: C, 66.89; H, 5.96; N, 4.88; O, 22.27. Found: C, 66.93; H, 6.00; N, 4.91; O, 22.30.

*4-{[(1,3-Dioxo-1,3-dihydro-2H-inden-2-ylidene)methyl]amino}-benzoic acid (**4b**)*

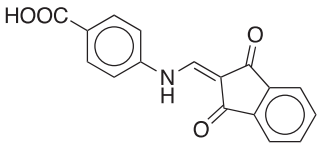

Yield 70%, m.p. 320–321°C; IR (ν, cm^{-1}): 3440 (N–H), 3200–2900 (COO–H), 3012 (=C–H), 1755 (C=O); ^{1}H NMR (300 MHz, DMSO): δ 11.30 (d, 1H), 8.36 (d, 1H), 7.94 (s, 1H), 7.92 (d, 2H), 7.65 (d, 2H), 7.60–7.50 (m, 4H); ^{13}C NMR (75 MHz, DMSO): δ 191.95, 189.63, 167.33, 144.30, 140.18, 134.94, 131.52, 127.89, 122.52, 122.19, 118.62, 107.27. Calculated for $C_{17}H_{11}NO_4$: C, 69.62; H, 3.78; N, 4.78; O, 21.82. Found: C, 69.65; H, 3.82; N, 4.80; O, 21.86.

*4-{[(1,3-Dimethyl-2,4,6-trioxotetrahydropyrimidin-5-(2H)-ylidene)-methyl]amino}benzoic acid (**4c**)*

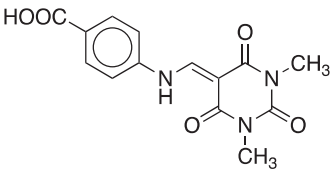

Yield 70%, m.p. 330–331°C; IR (ν, cm^{-1}): 3435 (N–H), 3200–2900 (COO–H), 3042 (=C–H), 1740 (C=O); ^{1}H NMR (300 MHz, DMSO): δ 12.62 (d, 1H), 8.60 (d, 1H), 7.93 (d, 2H), 7.59 (s, 2H), 2.06 (s, 6H); ^{13}C NMR (75 MHz, DMSO): δ 169.4, 160.30, 150.6, 149.6, 147.9, 131.68, 120.23, 116.80, 104.30, 29.4. Calculated for $C_{14}H_{13}N_3O_5$: C, 55.45; H, 4.32; N, 13.86; O, 26.38. Found: C, 54.49; H, 4.36; N, 13.91; O, 26.42.

*4-{[(2,4,6-Trioxotetrahydropyrimidin-5-(2H)-ylidene)methyl]amino}-benzoic acid (**4d**)*

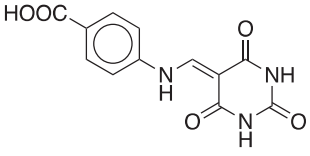

Yield 75%, m.p. 245–246°C; IR (ν, cm^{-1}): 3451 (N–H), 3200–2900 (COO–H), 3085 (=C–H), 1740 (C=O); ^{1}H NMR (300 MHz, DMSO): δ 11.91 (d, 1H), 11.09 (s, 1H), 10.90 (s, 1H), 8.58 (d, 1H), 7.94 (d, 2H), 7.60 (d, 2H); ^{13}C NMR (75 MHz, DMSO): δ 167.29, 166.70, 164.13, 151.57, 151.32, 142.78, 131.68, 128.23, 118.80, 94.30. Calculated for $C_{12}H_9N_3O_5$: C, 52.37; H, 3.30; N, 15.27; O, 29.07. Found: C, 52.39; H, 3.35; N, 15.31; O, 29.10.

*4-{[(2,6-Dioxocyclohexylidene)methyl]amino}benzoic acid (**4e**)*

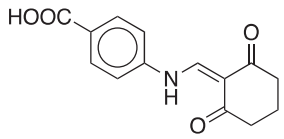

Yield 70%, m.p. 280–281°C; IR (ν, cm^{-1}): 3490 (N–H), 3200–2900 (COO–H), 3088 (=C–H), 1750 (C=O); ^{1}H NMR (300 MHz, DMSO): δ 11.77 (d, 1H), 8.29 (d, 1H), 7.92 (d, 1H), 7.64 (d, 2H), 2.48 (d, 2H), 2.06 (d, 2H), 1.19 (s, 2H); ^{13}C NMR (75 MHz, DMSO): δ 205.41, 201.86, 167.23, 147.00, 142.71, 131.50, 128.61, 119.17, 109.71, 34.46, 33.91, 31.38. Calculated for $C_{14}H_{13}NO_4$: C, 64.86; H, 5.05; N, 5.40; O, 24.68. Found: C, 64.90; H, 5.44; N, 5.43; O, 24.68.

*4-{[(2,2-Dimethyl-4,6-dioxo-1,3-dioxan-5-ylidene)methyl]amino}-benzoic acid (**4f**)*

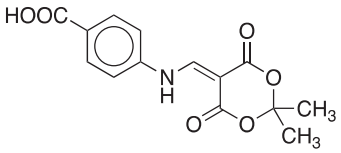

Yield 78%, m.p. 235–236°C; IR (ν, cm^{-1}): 3480 (N–H), 3200–2900 (COO–H), 3090 (=C–H), 1755 (C=O); ^{1}H NMR (300 MHz, DMSO): δ 11.24 (d, 1H), 8.60 (d, 1H), 7.93 (d, 2H), 7.58 (d, 2H), 1.62 (s, 6H); ^{13}C NMR (75 MHz, DMSO): δ 167.38, 164.55, 163.55, 153.62, 142.63, 131.61, 128.58, 119.27, 105.21, 88.38, 27.09. Calculated for $C_{14}H_{13}NO_6$: C, 57.73; H, 4.50; N, 4.81; O, 32.96. Found: C, 57.76; H, 4.53; N, 4.85; O, 33.00.

*4-{[(2,6-Dioxo-4-(tetrahydrofuran-2-yl)cyclohexylidene)methyl]-amino}benzoic acid (**4g**)*

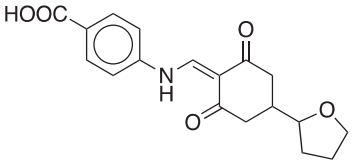

Yield 68%, m.p. 261–262°C; IR (ν, cm^{-1}): 3475 (N–H), 3200–2900 (COO–H), 3092 (=C–H), 1750 (C=O); ^{1}H NMR (300 MHz, DMSO): δ 12.61 (d, 1H), 8.51 (d, 1H), 7.91 (d, 2H), 7.60 (d, 2H), 3.75–3.70 (m, 3H), 3.02–2.70 (d, 4H), 2.25 (m, 1H), 1.90–170 (m, 4H); ^{13}C NMR (75 MHz, DMSO): δ 198.70, 194.65, 167.26, 156.80, 150.41, 142.68, 131.68, 128.54, 119.01, 110.55, 105.68, 92.20, 71.50, 42.66, 34.32, 33.12, 26.54. Calculated for $C_{18}H_{19}NO_5$: C, 65.64; H, 5.82; N, 4.25; O, 24.29. Found: C, 65.68; H, 5.85; N, 4.29; O, 24.32.

4.1.3 | General procedure for the preparation of the tetrahydroisoquinolynyl-benzoic acid derivatives 6a–g

Methylene-aminobenzoic acid derivatives (1 mmol) and ethyl cyanoacetate (1.2 mmol) were dissolved in DMF. Potassium *tert*-butoxide (KOT, 2 mmol) was added to the mixture. The reaction was allowed to proceed for 5 h at room temperature. After completion of the reaction, ice-cold water was added to the reaction flask. The mixture was acidified by HCl and the precipitate was filtered by vacuum filtration. Then, it was washed with water and dried in a vacuum oven. The product was purified by crystallization in acetone.

*4-[4-(Ethoxycarbonyl)-6,6-dimethyl-3,8-dioxo-5,6,7,8-tetrahydroisoquinolin-2-(3H)-yl]benzoic acid (**6a**)*

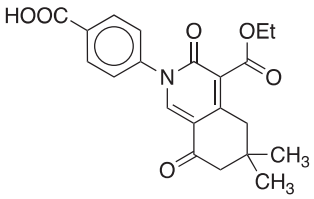

Yield 72%, m.p. 265–266°C; IR (ν, cm^{-1}): 3200–2900 (COO–H), 3092 (=C–H), 1748 (C=O); ^{1}H NMR (300 MHz, DMSO): δ 8.50 (s, 1H), 8.12 (d, 2H), 7.60 (d, 2H), 4.22 (q, 2H), 2.86 (s, 2H), 1.88 (s, 2H), 1.32 (t, 3H), 1.12 (s, 6H); ^{13}C NMR (75 MHz, DMSO): δ 194.03, 167.29, 164.33, 161.12, 159.60, 141.82, 140.79, 132.26, 131.50, 129.18, 121.62, 119.43, 61.36, 53.88, 42.35, 37.80, 28.26, 14.80. Calculated for $C_{21}H_{23}NO_5$: C, 68.28; H, 6.28; N, 3.79; O, 21.65. Found: C, 68.32; H, 6.31; N, 3.82; O, 21.69.

*4-[4-(Ethoxycarbonyl)-3,9-dioxo-3,9-dihydro-2H-indeno-(2,1-c)-pyridin-2-yl]benzoic acid (**6b**)*

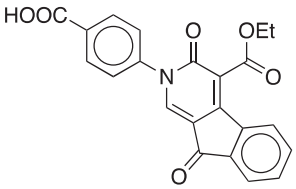

Yield 73%, m.p. 290–291°C; IR (ν, cm^{-1}): 3200–2900 (COO–H), 3082 (=C–H), 1742 (C=O); ^{1}H NMR (300 MHz, DMSO): δ 8.47 (s, 1H), 7.98 (d, 2H), 7.63 (d, 2H), 7.38–7.30 (m, 4H), 4.20 (q, 2H), 1.24 (t, 3H); ^{13}C NMR (75 MHz, DMSO): δ 187.62, 172.21, 164.30, 162.19, 160.01, 141.18, 138.10, 136.23, 135.62, 134.74, 133.81, 133.23, 131.73, 129.22, 124.12, 124.07, 117.07, 111.05, 61.35, 14.78. Calculated for $C_{22}H_{15}NO_6$: C,

67.87; H, 3.88; N, 3.60; O, 24.65. Found: C, 67.91; H, 3.91; N, 3.64; O, 24.69.

*4-[8-(Ethoxycarbonyl)-1,3-dimethyl-2,4,7-trioxo-1,3,4,7-tetrahydropyrido-(4,3-d)-pyrimidin-6-(2H)-yl]benzoic acid (**6c**)*

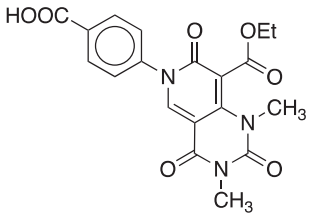

Yield 82%, m.p. 255–256°C; IR (ν, cm^{-1}): 3112 (=C–H), 1680 (C=O); ^{1}H NMR (300 MHz, DMSO): δ 8.52 (s, 1H), 7.93 (d, 2H), 7.60 (d, 2H), 4.16 (q, 2H), 2.76 (s, 3H), 2.70 (s, 3H), 1.32 (t, 3H); ^{13}C NMR (75 MHz, DMSO): δ 172.24, 167.24, 165.47, 157.58, 154.11, 147.73, 138.64, 136.26, 128.40, 125.88, 120.25, 118.92, 103.30, 62.39, 34.55, 28.34, 14.8. Calculated for $C_{19}H_{17}N_3O_7$: C, 57.14; H, 4.29; N, 10.52; O, 28.04. Found: C, 57.18; H, 4.32; N, 10.56; O, 28.07.

*4-[8-(Ethoxycarbonyl)-2,4,7-trioxo-1,3,4,7-tetrahydropyrido-(4,3-d)-pyrimidin-6-(2H)-yl]benzoic acid (**6d**)*

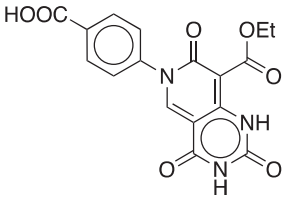

Yield 78%, m.p. 245–246°C; IR (ν, cm^{-1}): 3340 (N–H), 3110 (=C–H), 1688 (C=O); ^{1}H NMR (300 MHz, DMSO): δ 11.89 (s, 1H), 11.02 (s, 1H), 8.28 (s, 1H), 8.04 (d, 2H), 7.80 (d, 2H), 4.21 (q, 2H), 1.52 (t, 3H); ^{13}C NMR (75 MHz, DMSO): δ 178.28, 167.24, 165.47, 158.58, 157.11, 147.73, 138.64, 137.21, 128.40, 125.88, 120.25, 118.92, 104.24, 62.66, 15.39. Calculated for $C_{17}H_{13}N_3O_7$: C, 54.99; H, 3.53; N, 11.32; O, 30.16. Found: C, 55.03; H, 3.57; N, 11.36; O, 30.18.

*4-[4-(Ethoxycarbonyl)-3,8-dioxo-5,6,7,8-tetrahydroisoquinolin-2-(3H)-yl]benzoic acid (**6e**)*

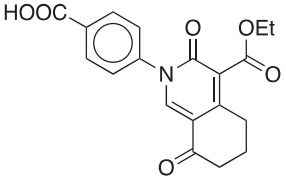

Yield 75%, m.p. 280–281°C; IR (ν, cm^{-1}): 3150 (=C–H), 1690 (C=O); ^{1}H NMR (300 MHz, DMSO): δ 8.50 (s, 1H), 8.13 (d, 2H), 7.92 (d, 2H), 4.21 (q, 2H), 2.86 (t, 2H), 2.11 (d, 2H), 1.48 (m, 2H), 1.33 (t, 3H); ^{13}C NMR (75 MHz, DMSO): δ 194.16, 167.26, 164.35, 163.01, 159.30, 141.86, 141.12, 132.26, 131.33, 129.18, 121.68, 119.39, 61.36, 39.48, 29.64, 21.18, 14.78. Calculated for $C_{19}H_{17}NO_6$: C, 64.22; H, 4.82; N, 3.94; O, 27.01. Found: C, 64.25; H, 4.86; N, 3.98; O, 27.05.

*4-[8-(Ethoxycarbonyl)-2,2-dimethyl-7-oxo-4H-(1,3)-dioxino(5,4-c)-pyridin-6-(7H)-yl]benzoic acid (**6f**)*

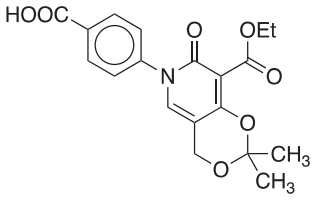

Yield 70%, m.p. 281–282°C; IR (ν, cm^{-1}): 3110 (=C–H), 1690 (C=O); ^{1}H NMR (300 MHz, DMSO): δ 8.45 (s, 1H), 8.11 (d, 2H), 7.81 (d, 2H), 4.23 (q, 2H), 1.78 (s, 6H), 1.30 (t, 3H); ^{13}C NMR (75 MHz, DMSO): δ 171.03, 168.85, 166.27, 163.81, 162.80, 147.89, 141.21, 130.42, 125.24, 120.32, 108.09, 101.54, 96.32, 61.62, 25.42, 14.74. Calculated for $C_{19}H_{19}NO_7$: C, 61.12; H, 5.13; N, 3.75; O, 30.00. Found: C, 61.16; H, 5.17; N, 3.79; O, 30.03.

*4-[4-(Ethoxycarbonyl)-3,8-dioxo-6-(tetrahydrofuran-2-yl)-5,6,7,8-tetrahydroisoquinolin-2-(3H)-yl]benzoic acid (**6g**)*

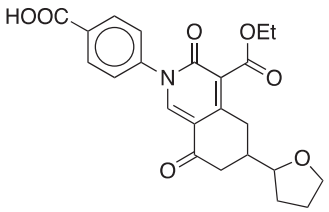

Yield 75%, m.p. 290–291°C; IR (ν, cm^{-1}): 3110 (=C–H), 1680 (C=O); ^{1}H NMR (300 MHz, DMSO): δ 8.43 (s, 1H), 7.98 (d, 2H), 7.80 (d, 2H), 4.21 (q, 2H), 3.80 (t, 2H), 2.80 (2, 2H), 1.70–2.10 (m, 7H), 1.26 (t, 3H); ^{13}C NMR (75 MHz, DMSO): δ 194.5, 169.41, 167.20, 165.21, 156.80, 138.21, 137.41, 130.51, 125.91, 121.55, 121.1, 119.22, 93.30, 71.51, 61.14, 43.41, 41.44, 33.72, 31.22, 26.21, 14.22. Calculated for $C_{22}H_{23}NO_6$: C, 66.49; H, 5.83; N, 3.52; O, 24.15. Found: C, 66.53; H, 5.86; N, 3.55; O, 24.18.

4.2 | Biological studies

4.2.1 | AChE activity assay

AChE from *Electrophorus electricus* (C2888, Type V-S), which is a tetramer composed of four equal subunits of 70 kDa each, 5,5′-dithiobis(2-nitrobenzoic acid) (DTNB; $C_{14}H_8N_2O_8S_2$, D8130), and

acetylthiocholine iodide (AChI; $C_7H_{16}INOS$, 01480) were acquired from Sigma-Aldrich Chemie GmbH. In vitro effects on the AChE activity of the newly synthesized methylene-aminobenzoic acid and tetrahydroisoquinolynyl-benzoic acid derivatives (**4a**–**g** and **6a**–**g**) were evaluated by the assay of Ellman et al.,[47] using AChI as the substrate at 412 nm. One enzyme unit (EU) was defined as the hydrolysis of 1.0 μmol ACh to choline and acetate per minute at pH 8.0 and temperature 37°C. TAC ($C_{13}H_{14}N_2$, 1,2,3,4-tetrahydroacridin-9-amine, A3773) was used as the reference drug. All the measurements were repeated three times. The analysis results were expressed as means of triplicate assays ± SEM.

4.2.2 | CA activity assay

The media used for affinity chromatography (4B200, Sepharose 4B, fractionation range 30–50 kDa), and all chemical reagents, including 4-nitrophenyl acetate ($C_8H_6NO_4$, N8130), were of analytical grade and were commercially acquired from Sigma-Aldrich Chemie GmbH. Prestained protein molecular weight (MW) standard and markers (proteins ranging from 10 to 250 kDa, 26620) were purchased from Thermo Fisher Scientific Inc. Human erythrocyte samples were supplied by the Faculty of Medicine, Research Hospital, Atatürk University (Erzurum, Turkey). The experimental protocol was confirmed by the Ethics Committee for Clinical Research of Faculty of Medicine, Atatürk University (Erzurum, Turkey). hCA isoenzymes (I and II) were obtained with purification from human erythrocytes by Sepharose-4B-L-tyrosine-sulfanilamide affinity chromatography. The protein concentration of the eluates was determined by a simple analytical procedure at 595 nm, according to the Bradford assay,[48,49] spectrophotometrically.[50] The purity of the hCA I and II isoforms was controlled with 3–8% discontinued sodium dodecyl sulfate-polyacrylamide gel electrophoresis, as explained by Laemmli.[51,52] The MW of these hCA isoenzymes was computed by this method as well as with the SynGene imaging tool, which was approximately 29 kDa.[53] The esterase activity of the hCA isoforms was determined by following the change in absorbance at 348 nm over 3 min[54] according to the method described by Verpoorte et al.[55] One enzyme unit (EU) was defined as the hydrolysis of 1.0 μmol 4-nitrophenyl acetate to 4-nitrophenyl per minute at pH 7.4 and temperature 25°C. AAZ ($C_4H_6N_4O_3S_2$, *N*-(5-sulfamoyl-1,3,4-thiadiazol-2-yl)acetamide, PHR1908) was used as the reference drug. All rate measurements were repeated three times. The assay results were expressed as means of triplicate tests ± SEM.

4.2.3 | AChE and CA kinetic analysis

To investigate the in vitro inhibitory mechanisms of the novel synthesized methylene-aminobenzoic acid and tetrahydroisoquinolynyl-benzoic acid analogs (**4a**–**g** and **6a**–**g**), kinetic studies were performed with the variable substrate and analog concentrations, and IC_{50} plots,[56,57] Michaelis–Menten curves,[58,59] and Lineweaver–Burk plots[60,61] were generated. Solutions of the synthesized methylene-aminobenzoic acid and tetrahydroisoquinolynyl-benzoic acid derivatives (**4a**–**g** and **6a**–**g**), TAC, and AAZ were prepared in DMSO (C_2H_6SO, D8418) at an initial concentration of 1 mg/ml. The concentration of DMSO in the final reaction mixture was approximately 1%. From the obtained data, IC_{50}, V_{max}, K_m, and K_I values for these benzoic acid analogs (**4a**–**g** and **6a**–**g**) were calculated, and the types of inhibition of AChE and hCA isoenzymes were determined, as previously reported by Türkeş et al.[62–65]

4.3 | In silico studies

4.3.1 | ADME–Tox study

Novel synthesized methylene-aminobenzoic acid and tetrahydroisoquinolynyl-benzoic acid derivatives (**4a**–**g** and **6a**–**g**) were subjected to ADME–Tox prediction[66] using the QikProp module[67] of Schrödinger 2020-2 for Mac (Schrödinger LLC). The module provided data such as molecular weight of the analogs (**4a**–**g** and **6a**–**g**), the computed dipole moment of the derivatives, total solvent-accessible volume in $Å^3$ using a probe with a 1.4-Å radius, octanol/gas partition coefficient, water/gas partition coefficient, octanol/water partition coefficient, aqueous solubility, IC_{50} value for the blockage of HERG K^+ channels, apparent Caco-2 cell permeability in nm/s, brain/blood partition coefficient, apparent MDCK cell permeability in nm/s, skin permeability, prediction of binding to human serum albumin, HOA, and van der Waals surface area of polar nitrogen and oxygen atoms. Moreover, the number of violations of Lipinski's rule of five[68] and Jorgensen's rule of three[69] was investigated. Also, the PAINS alert[70] was evaluated using the SwissADME platform.

4.3.2 | Molecular docking study

The molecular docking study was carried out using panels (i.e., Maestro,[71] Protein Preparation Wizard,[72] LigPrep,[73] Receptor Grid Generation,[74] and Prime MM-GBSA[75]) in the Schrödinger Suite 2020-2 for Mac. The three-dimensional (3D) crystal structures of ligand-bound HI6 (PDB ID: 5HF9 for AChE),[76] GZH (PDB ID: 6I0L for hCA I),[77] and GTQ (PDB ID: 4E3D for hCA II)[46] were retrieved from the Protein Data Bank[78] and were prepared utilizing the Protein Preparation Wizard.[79] The 3D structures of novel synthesized methylene-aminobenzoic acid and tetrahydroisoquinolynyl-benzoic acid derivatives (**4a**–**g** and **6a**–**g**) were sketched by ChemDraw[80] version 19.0 for Mac (PerkinElmer Inc.). They were suitably optimized for their ionization states at pH 7.4 ± 0.5[81] with Epik[82] in the OPLS3e force field[83] using the LigPrep module[84] with default settings. The Receptor Grid Generation tool[85] was used to generate the grid for docking in the 5HF9, 6I0L, and 4E3D. All of these ligands (**4a**–**g** and **6a**–**g**) were docked utilizing the Glide extra precision (XP) scoring function.[86] Furthermore, the docked poses were rescored

using the MM-GBSA approach[87] to assess the electrostatic contribution of the VSGB solvation model[88] with the OPLS3 force field.[89]

4.4 | Statistical studies

The analysis of the data and drawing of graphs were realized using GraphPad Prism version 7 for Mac (GraphPad Software). The inhibition constants were calculated by SigmaPlot version 12 for Windows (Systat Software). The fit of enzyme inhibition models was compared using the extra sum-of-squares *F* test and the AICc approach. The results were exhibited as mean ± SEM (95% confidence intervals). Differences between data sets were considered statistically significant when $p < .05$.

ACKNOWLEDGMENTS

This study was supported by the Research Fund of Sakarya University (Grant Number: 2018-2-7-307), the Research Fund of Erzincan Binali Yıldırım University (Grant Number: FBA-2017-501), the Research Fund of Ardahan University (Grant Number: 2019-007), and the Research Fund of Anadolu University (Grant Number: 1610S681).

CONFLICTS OF INTERESTS

The authors declare that there are no conflicts of interests.

ORCID

Cüneyt Türkeş https://orcid.org/0000-0002-2932-2789
Mustafa Arslan https://orcid.org/0000-0003-0796-4374

REFERENCES

[1] S. K. Chaturvedi, M. K. Siddiqi, P. Alam, R. H. Khan, *Process Biochem. (Amsterdam, Neth.)* **2016**, *51*, 1183. https://doi.org/10.1016/j.procbio.2016.05.015
[2] R. H. Khan, M. K. Siddiqi, V. N. Uversky, P. Salahuddin, *Int. J. Biol. Macromol.* **2019**, *127*, 250. https://doi.org/10.1016/j.ijbiomac.2018.12.271
[3] M. Sharifi, M. J. Sohrabi, S. H. Hosseinali, A. Hasan, P. H. Kani, A. J. Talaei, A. Y. Karim, N. M. Q. Nanakali, A. Salihi, F. M. Aziz, *Int. J. Biol. Macromol.* **2020**, *143*, 665. https://doi.org/10.1016/j.ijbiomac.2019.12.064
[4] M. Zaman, A. N. Khan, S. M. Zakariya, R. H. Khan, *Int. J. Biol. Macromol.* **2019**, *134*, 1022. https://doi.org/10.1016/j.ijbiomac.2019.05.109
[5] L. P. Köse, I. Gülcin, A. C. Gören, J. Namiesnik, A. L. Martinez-Ayala, S. Gorinstein, *Ind. Crops Prod.* **2015**, *74*, 712. https://doi.org/10.1016/j.indcrop.2015.05.034
[6] E. Bursal, P. Taslimi, A. C. Gören, İ. Gülçin, *Biocatal. Agric. Biotechnol.* **2020**, *28*, 101711. https://doi.org/10.1016/j.bcab.2020.101711
[7] Y. Demir, E. Oruç, A. Topal, *Hacettepe J. Biol. Chem.* **2016**, *44*, 515. https://doi.org/10.15671/HJBC.2016.132
[8] C. Caglayan, P. Taslimi, C. Türk, I. Gulcin, F. M. Kandemir, Y. Demir, Ş. Beydemir, *Environ. Sci. Pollut. Res.* **2020**, *27*, 10607. https://doi.org/10.1007/s11356-020-07611-z
[9] E. Hoff, D. Zou, S. Schiza, Y. Demir, L. Grote, I. Bouloukaki, Ş. Beydemir, D. Eskandari, K. Stenlöf, J. Hedner, *J. Sleep Res.* **2020**, *29*, e12956. https://doi.org/10.1111/jsr.12956
[10] P. Taslimi, F. M. Kandemir, Y. Demir, M. İleritürk, Y. Temel, C. Caglayan, İ. Gulçin, *J. Biochem. Mol. Toxicol.* **2019**, *33*, e22313. https://doi.org/10.1002/jbt.22313
[11] A. Topal, M. Atamanalp, E. Oruç, Y. Demir, Ş. Beydemir, A. Işık, *Arch. Ind. Hyg. Toxicol.* **2014**, *65*, 377. https://doi.org/10.2478/10004-1254-65-2014-2547
[12] I. Gulcin, S. Beydemir, *Mini-Rev. Med. Chem.* **2013**, *13*, 408. https://doi.org/10.2174/138955713804999874
[13] K. Kucukoglu, H. I. Gul, P. Taslimi, I. Gulcin, C. T. Supuran, *Bioorg. Chem.* **2019**, *86*, 316. https://doi.org/10.1016/j.bioorg.2019.02.008
[14] K. M. Hanson, E. Gratton, C. J. Bardeen, *Free Radic. Biol. Med.* **2006**, *41*, 1205. https://doi.org/10.1016/j.freeradbiomed.2006.06.011
[15] M. E. Crisan, P. Bourosh, M. E. Maffei, A. Forni, S. Pieraccini, M. Sironi, Y. M. Chumakov, *PLOS One* **2014**, *9*, e101892. https://doi.org/10.1371/journal.pone.0101892
[16] R. Richards, D. Xing, *J. Pharm. Biomed. Anal.* **1994**, *12*, 1063. https://doi.org/10.1016/0731-7085(94)00056-5
[17] J. Correa-Basurto, I. V. Alcántara, L. M. Espinoza-Fonseca, J. G. Trujillo-Ferrara, *Eur. J. Med. Chem.* **2005**, *40*, 732. https://doi.org/10.1016/j.ejmech.2005.03.011
[18] M. Krátký, K. Konečná, J. Janoušek, M. Brablíková, O. Janďourek, F. Trejtnar, J. Stolaříková, J. Vinšová, *Biomolecules* **2020**, *10*, 9. https://doi.org/10.3390/biom10010009
[19] E.-S. M. Abdel-Hafez, G. E.-D. A. Abuo-Rahma, M. Abdel-Aziz, M. F. Radwan, H. H. Farag, *Bioorg. Med. Chem.* **2009**, *17*, 3829. https://doi.org/10.1016/j.bmc.2009.04.037
[20] P. Chand, P. L. Kotian, P. E. Morris, S. Bantia, D. A. Walsh, Y. S. Babu, *Bioorg. Med. Chem.* **2005**, *13*, 2665. https://doi.org/10.1016/j.bmc.2005.01.042
[21] C. W. Phoon, P. Y. Ng, A. E. Ting, S. L. Yeo, M. M. Sim, *Bioorg. Med. Chem. Lett.* **2001**, *11*, 1647. https://doi.org/10.1016/S0960-894X(01)00263-3
[22] S. R. Hussaini, R. R. Chamala, Z. Wang, *Tetrahedron* **2015**, *36*, 6017. https://doi.org/10.1016/j.tet.2015.06.026
[23] P. Singh, P. Sharma, K. Bisetty, M. P. Mahajan, *Tetrahedron* **2009**, *65*, 8478. https://doi.org/10.1016/j.tet.2009.08.038
[24] A. K. Chattopadhyay, S. Hanessian, *Chem. Commun.* **2015**, *51*, 16437. https://doi.org/10.1039/C5CC05891K
[25] I. O. Edafiogho, S. B. Kombian, K. V. Ananthalakshmi, N. N. Salama, N. D. Eddington, T. L. Wilson, M. S. Alexander, P. L. Jackson, C. D. Hanson, K. Scott, *J. Pharm. Sci.* **2007**, *96*, 2509. https://doi.org/10.1002/jps.20967
[26] A. Nocentini, A. Bonardi, P. Gratteri, B. Cerra, A. Gioiello, C. T. Supuran, *J. Enzyme Inhib. Med. Chem.* **2018**, *33*, 1453. https://doi.org/10.1080/14756366.2018.1512597
[27] K. D'Ambrosio, S. Carradori, S. M. Monti, M. Buonanno, D. Secci, D. Vullo, C. T. Supuran, G. De Simone, *Chem. Commun.* **2015**, *51*, 302. https://doi.org/10.1039/C4CC07320G
[28] A. Maresca, C. Temperini, H. Vu, N. B. Pham, S.-A. Poulsen, A. Scozzafava, R. J. Quinn, C. T. Supuran, *J. Am. Chem. Soc.* **2009**, *131*, 3057. https://doi.org/10.1021/ja809683v
[29] H. B. Broughton, I. A. Watson, *J. Mol. Graphics Modell.* **2004**, *23*, 51. https://doi.org/10.1016/j.jmgm.2004.03.016
[30] L. Duchet, J. C. Legeay, D. Carrié, L. Paquin, J. J. V. Eynde, J. P. Bazureau, *Tetrahedron* **2010**, *66*, 986. https://doi.org/10.1016/j.tet.2009.11.079
[31] S. Batra, Y. A. Sabnis, P. J. Rosenthal, M. A. Avery, *Bioorg. Med. Chem.* **2003**, *11*, 2293. https://doi.org/10.1016/S0968-0896(03)00117-2
[32] G. Bringmann, *Alkaloids* **1986**, *29*, 141.
[33] J. A. Eremina, E. V. Lider, T. S. Sukhikh, I. V. Eltsov, N. V. Kuratieva, B. A. Zakharov, L. A. Sheludyakova, L. S. Klyushova, E. A. Ermakova, V. V. Dotsenko, *Polyhedron* **2020**, *178*, 178. https://doi.org/10.1016/j.poly.2019.114325

[34] C. Oliveira, F. Cagide, J. Teixeira, R. Amorim, L. Sequeira, F. Mesiti, T. Silva, J. Garrido, F. Remião, S. Vilar, *Front. Chem.* **2018**, *6*, 126. https://doi.org/10.3389/fchem.2018.00126

[35] C. Oliveira, D. Bagetta, F. Cagide, J. Teixeira, R. Amorim, T. Silva, J. Garrido, F. Remião, E. Uriarte, P. J. Oliveira, *Eur. J. Med. Chem.* **2019**, *174*, 116. https://doi.org/10.1016/j.ejmech.2019.04.026

[36] P. Anand, B. Singh, *Bioorg. Med. Chem.* **2012**, *20*, 521. https://doi.org/10.1016/j.bmc.2011.05.027

[37] A. M. Mohsen, A. Salama, A. A. Kassem, *J. Drug Deliv. Sci. Technol.* **2020**, *59*, 101910. https://doi.org/10.1016/j.jddst.2020.101910

[38] W. M. Eldehna, A. Nocentini, Z. M. Elsayed, T. Al-Warhi, N. Aljaeed, O. J. Alotaibi, M. M. Al-Sanea, H. A. Abdel-Aziz, C. T. Supuran, *ACS Med. Chem. Lett.* **2020**, *11*, 1022. https://doi.org/10.1021/acsmedchemlett.0c00094

[39] A.-M. Alaa, A. S. El-Azab, M. Ceruso, C. T. Supuran, *Bioorg. Med. Chem. Lett.* **2014**, *24*, 5185. https://doi.org/10.1016/j.bmcl.2014.09.076

[40] G. Rotondi, P. Guglielmi, S. Carradori, D. Secci, C. De Monte, B. De Filippis, C. Maccallini, R. Amoroso, R. Cirilli, A. Akdemir, *J. Enzyme Inhib. Med. Chem.* **2019**, *34*, 1400. https://doi.org/10.1080/14756366.2019.1651315

[41] V. Alterio, A. Di Fiore, K. D'Ambrosio, C. T. Supuran, G. De Simone, *Chem. Rev.* **2012**, *112*, 4421. https://doi.org/10.1021/cr200176r

[42] G. Çelik, T. Arslan, M. Şentürk, D. Ekinci, *Arch. Pharm.* **2020**, *353*, 1900292. https://doi.org/10.1002/ardp.201900292

[43] N. Berber, M. Arslan, Ç. Bilen, Z. Sackes, N. Gencer, O. Arslan, *Russ. J. Bioorg. Chem.* **2015**, *41*, 414. https://doi.org/10.1134/S1068162015040111

[44] J.-Y. Winum, A. Scozzafava, J.-L. Montero, C. T. Supuran, *Curr. Pharm. Des.* **2008**, *14*, 615. https://doi.org/10.2174/138161208783877848

[45] A. Innocenti, D. Vullo, A. Scozzafava, C. T. Supuran, *Bioorg. Med. Chem.* **2008**, *16*, 7424. https://doi.org/10.1016/j.bmc.2008.06.013

[46] D. P. Martin, S. M. Cohen, *Chem. Commun.* **2012**, *48*, 5259. https://doi.org/10.1039/C2CC32013D

[47] G. L. Ellman, K. D. Courtney, V. Andres Jr, R. M. Featherstone, *Biochem. Pharmacol.* **1961**, *7*, 88. https://doi.org/10.1016/0006-2952(61)90145-9

[48] C. Türkeş, Y. Demir, Ş. Beydemir, *Appl. Biochem. Biotechnol.* **2019**, *189*, 318. https://doi.org/10.1007/s12010-019-03009-x

[49] İ. Gulçin, P. Taslimi, A. Aygün, N. Sadeghian, E. Bastem, O. I. Kufrevioglu, F. Turkan, F. Şen, *Int. J. Biol. Macromol.* **2018**, *119*, 741. https://doi.org/10.1016/j.ijbiomac.2018.08.001

[50] M. M. Bradford, *Anal. Biochem.* **1976**, *72*, 248. https://doi.org/10.1016/0003-2697(76)90527-3

[51] U. K. Laemmli, *Nature* **1970**, *227*, 680. https://doi.org/10.1038/227680a0

[52] P. Taslimi, H. E. Aslan, Y. Demir, N. Oztaskin, A. Maraş, İ. Gulçin, S. Beydemir, S. Goksu, *Int. J. Biol. Macromol.* **2018**, *119*, 857. https://doi.org/10.1016/j.ijbiomac.2018.08.004

[53] L. Wang, C. E. Sparacino-Watkins, J. Wang, N. Wajih, P. Varano, Q. Xu, E. Cecco, J. Tejero, M. Soleimani, D. B. Kim-Shapiro, *Br. J. Pharmacol.* **2020**, *177*, 898. https://doi.org/10.1111/bph.14887

[54] B. Arabaci, I. Gulcin, S. Alwasel, *Molecules* **2014**, *19*, 10103. https://doi.org/10.3390/molecules190710103

[55] J. A. Verpoorte, S. Mehta, J. T. Edsall, *J. Biol. Chem.* **1967**, *242*, 4221.

[56] Y. Akbaba, C. Türkeş, L. Polat, H. Söyüt, E. Şahin, A. Menzek, S. Göksu, Ş. Beydemir, *J. Enzyme Inhib. Med. Chem.* **2013**, *28*, 1073. https://doi.org/10.3109/14756366.2012.715287

[57] C. Türkeş, H. Söyüt, Ş. Beydemir, *Open J. Biochem.* **2013**, *1*, 10. https://doi.org/10.15764/BIOC.2014.01002

[58] K. A. Johnson, R. S. Goody, *Biochemistry* **2011**, *50*, 8264. https://doi.org/10.1021/bi201284u

[59] Y. Demir, *J. Pharm. Pharmacol.* **2019**, *71*, 1576. https://doi.org/10.1111/jphp.13144

[60] H. Lineweaver, D. Burk, *J. Am. Chem. Soc.* **1934**, *56*, 658. https://doi.org/10.1021/ja01318a036

[61] Y. Demir, *Drug Dev. Res.* **2020**, *81*, 628. https://doi.org/10.1002/ddr.21667

[62] C. Türkeş, H. Söyüt, Ş. Beydemir, *Pharmacol. Rep.* **2014**, *66*, 74. https://doi.org/10.1016/j.pharep.2013.08.007

[63] C. Türkeş, H. Söyüt, Ş. Beydemir, *J. Enzyme Inhib. Med. Chem.* **2015**, *30*, 622. https://doi.org/10.3109/14756366.2014.959511

[64] C. Türkeş, H. Söyüt, Ş. Beydemir, *Environ. Toxicol. Pharmacol.* **2016**, *42*, 252. https://doi.org/10.1016/j.etap.2015.11.024

[65] C. Türkeş, Y. Demir, Ş. Beydemir, *J. Biomol. Struct. Dyn.* **2020**, 1. https://doi.org/10.1080/07391102.2020.1806927

[66] S. Gündoğdu, C. Türkeş, M. Arslan, Y. Demir, Ş. Beydemir, *ChemistrySelect* **2019**, *4*, 13347. https://doi.org/10.1002/slct.201903458

[67] P. Taslimi, M. Işık, F. Türkan, M. Durgun, C. Türkeş, İ. Gülçin, Ş. Beydemir, *J. Biomol. Struct. Dyn.* **2020**, 1. https://doi.org/10.1080/07391102.2020.1790422

[68] C. A. Lipinski, F. Lombardo, B. W. Dominy, P. J. Feeney, *Adv. Drug Delivery Rev.* **1997**, *23*, 3. https://doi.org/10.1016/S0169-409X(96)00423-1

[69] E. M. Duffy, W. L. Jorgensen, *J. Am. Chem. Soc.* **2000**, *122*, 2878. https://doi.org/10.1021/ja993663t

[70] J. B. Baell, G. A. Holloway, *J. Med. Chem.* **2010**, *53*, 2719. https://doi.org/10.1021/jm901137j

[71] Y. Demir, C. Türkeş, Ş. Beydemir, *Anti-Cancer Agents Med. Chem.* **2020**, *20*, 887. https://doi.org/10.2174/1871520620666200218110645

[72] M. Işık, Y. Demir, M. Durgun, C. Türkeş, A. Necip, Ş. Beydemir, *Chem. Pap.* **2020**, *74*, 1395. https://doi.org/10.1007/s11696-019-00988-3

[73] Ş. Beydemir, C. Türkeş, A. Yalçın, *Drug Chem. Toxicol.* **2019**, 1. https://doi.org/10.1080/01480545.2019.1620266

[74] C. Türkeş, Y. Demir, Ş. Beydemir, *J. Biomol. Struct. Dyn.* **2020**, 1. https://doi.org/10.1080/07391102.2020.1736631

[75] M. Işık, Ş. Beydemir, Y. Demir, M. Durgun, C. Türkeş, A. Nasır, A. Necip, M. Akkuş, *Int. J. Biol. Macromol.* **2020**, *146*, 1111. https://doi.org/10.1016/j.ijbiomac.2019.09.237

[76] M. C. Franklin, M. J. Rudolph, C. Ginter, M. S. Cassidy, J. Cheung, *Proteins: Struct., Funct., Bioinf.* **2016**, *84*, 1246. https://doi.org/10.1002/prot.25073

[77] M. Bozdag, M. Ferraroni, C. Ward, F. Carta, S. Bua, A. Angeli, S. P. Langdon, I. H. Kunkler, A.-M. S. Al-Tamimi, C. T. Supuran, *Eur. J. Med. Chem.* **2019**, *182*, 111600. https://doi.org/10.1016/j.ejmech.2019.111600

[78] C. Türkeş, Ş. Beydemir, *Appl. Biochem. Biotechnol.* **2020**, *190*, 252. https://doi.org/10.1007/s12010-019-03073-3

[79] C. Türkeş, *Protein Pept. Lett.* **2019**, *26*, 392. https://doi.org/10.2174/0929866526666190226162225

[80] M. Durgun, C. Türkeş, M. Işık, Y. Demir, A. Saklı, A. Kuru, A. Güzel, Ş. Beydemir, S. Akocak, S. M. Osman, Z. AlOthman, C. T. Supuran, *J. Enzyme Inhib. Med. Chem.* **2020**, *35*, 950. https://doi.org/10.1080/14756366.2020.1746784

[81] A. Kilic, L. Beyazsakal, M. Işık, C. Türkeş, A. Necip, K. Takım, Ş. Beydemir, *J. Organomet. Chem.* **2020**, *927*, 121542. https://doi.org/10.1016/j.jorganchem.2020.121542

[82] M. Işık, S. Akocak, N. Lolak, P. Taslimi, C. Türkeş, İ. Gülçin, M. Durgun, Ş. Beydemir, *Arch. Pharm.* **2020**, *353*, e2000102. https://doi.org/10.1002/ardp.202000102

[83] C. Türkeş, M. Arslan, Y. Demir, L. Cocaj, A. R. Nixha, Ş. Beydemir, *Bioorg. Chem.* **2019**, *89*, 103004. https://doi.org/10.1016/j.bioorg.2019.103004

[84] C. Türkeş, *J. Inst. Sci. Technol.* **2019**, *9*, 1013. https://doi.org/10.21597/jist.491054

[85] C. Türkeş, *J. Pharm. Pharmacol.* **2019**, *71*, 1553. https://doi.org/10.1111/jphp.13141

[86] C. Türkeş, Ş. Beydemir, Ö. İ. Küfrevioğlu, *ChemistrySelect* **2019**, *4*, 9731. https://doi.org/10.1002/slct.201902424

[87] N. Lolak, S. Akocak, C. Türkeş, P. Taslimi, M. Işık, Ş. Beydemir, İ. Gülçin, M. Durgun, *Bioorg. Chem.* **2020**, *100*, 103897. https://doi.org/10.1016/j.bioorg.2020.103897

[88] B. Sever, C. Türkeş, M. D. Altıntop, Y. Demir, Ş. Beydemir, *Int. J. Biol. Macromol.* **2020**, *163*, 1970. https://doi.org/10.1016/j.ijbiomac.2020.09.043

[89] Q. Istrefi, C. Türkeş, M. Arslan, Y. Demir, A. R. Nixha, Ş. Beydemir, Ö. İ. Küfrevioğlu, *Arch. Pharm.* **2020**, *353*, e1900383. https://doi.org/10.1002/ardp.201900383

SUPPORTING INFORMATION

Additional supporting information may be found online in the supporting information tab for this article.

How to cite this article: Kalaycı M, Türkeş C, Arslan M, Demir Y, Beydemir Ş. Novel benzoic acid derivatives: Synthesis and biological evaluation as multitarget acetylcholinesterase and carbonic anhydrase inhibitors. *Arch Pharm*. 2020;e2000282. https://doi.org/10.1002/ardp.202000282